DUAL CHANNEL BIDIRECTIONAL WAVELENGTH DIVISION MULTIPLEXING DATALINK

by

Henri Edouard Tohme

Thesis submitted to the Faculty of the

Virginia Polytechnic Institute and State University

in partial fulfillment of the requirements for the degree of

Master of Science

in

Electrical Engineering

APPROVED:

Ahmad Safaai-Jazi, Chairman

Richard O. Claus

Ronald J. Pieper

June 1988

Blacksburg, Virginia

DUAL CHANNEL BIDIRECTIONAL WAVELENGTH DIVISION MULTIPLEXING DATALINK

by

Henri Edouard Tohme

Ahmad Safaai-Jazi, Chairman

Electrical Engineering

(ABSTRACT)

Wavelength division multiplexing two channels on one fiber is one approach that enables us to make use of the extremely large bandwidth of optical fibers. We start with an analysis of optical fibers, sources, detectors, filters and wavelength division multiplexers. Then, using the knowledge from the experimental data, we design a 20 km bidirectional WDM datalink. The design is backed up with theory and measurements. Fiber to the home is one of many applications that makes use of such a design.

ACKNOWLEDGEMENTS

I would like to thank all those wonderful people who helped me prepare my thesis, especially and Dr Jazi. I also would like to thank my family, my relatives and my friends. I dedicate this thesis to all of you.

TABLE OF CONTENTS

1.0 INTRODUCTION 1

2.0 BASIC PRINCIPLES 5

3.0 BIDIRECTIONAL WDM DATALINK 14

4.0 FIBEROPTIC SOURCES 17

4.1 Principles of Operation of an LED 18

4.1.1 Experimental Measurements of the LED Spectrum 22

4.1.2 Design Configurations 25

4.1.3 Operating Parameters and Characteristics 29

4.1.4 Experimental Measurements 33

4.1.5 Temperature Dependence 36

4.2. Laser Diodes 39

4.2.1 Thermoelectric Devices 44

4.2.2 Experimental Results 49

5.0 PHOTODETECTORS 52

5.1 Pin Photodiodes 52

5.2 Avalanche Photodiodes 57

6.0 WAVELENGTH SELECTIVE COMPONENTS 59

6.1 Multimode Wavelength Division Multiplexers 59

6.2 Single Mode Wavelength Division Multiplexers 65

6.2.1 Coupled Mode Theory 68

6.2.2 Experimental Measurements of Single Mode WDM's ... 70

7.0 ATTENUATION 74

8.0 BANDWIDTH 76

9.0 SYSTEM DESIGN 80

9.1 System Specification 80

9.2 High Speed Channel Power and Bandwidth Budgets 83

9.3 Low Speed Channel Power and Bandwidth Budgets 84

9.4 Crosstalk Analysis 86

9.4.1 Crosstalk at the Distribution Center 87

9.4.2 Crosstalk at the Residence 93

10.0 CONCLUSIONS 96

REFERENCES 99

VITA 103

LIST OF ILLUSTRATIONS

Figure 1. Step index and graded index optical fibers .. 8

Figure 2. Total internal reflection and numercical aperture 9

Figure 3. Bidirectional WDM datalink 16

Figure 4. Electron recombination for (a) direct band gap material and (b) indirect band gap material 20

Figure 5. Output spectrum measurement system 23

Figure 6. Output spectrum of a 1520 nm LED which is coupled to a 9/125 μm fiber 24

Figure 7. Planar double heterojunction LED 26

Figure 8. Edge emitting LED 28

Figure 9. LED output power versus drive current 31

Figure 10. Rise and fall time of edge emitting LED 34

Figure 11. Rise and fall time of an edge emitting LED versus drive current 35

Figure 12. Output spectrum of an edge emitting LED with respect to temperature variations 37
Figure 13. Configuration of a laser diode 40
Figure 14. Output power versus drive current for a laser diode 42
Figure 15. Cross section of a typical thermoelectric cooler 45
Figure 16. Thermoelectric module assembly 48
Figure 17. Output spectrum of a 1310 nm Laser which is coupled to a 9/125 μm fiber 50
Figure 18. Output spectrum of a 1290 nm Laser which is coupled to a 9/125 μm fiber 51
Figure 19. PIN photodiode configuration 53
Figure 20. PIN diode responsivity 56
Figure 21. Avalanche photodiode configuration 58
Figure 22. Multimode WDM with Selfoc lens and dichroic filter 60
Figure 23. Spectral response of a 1300 nm dichroic band pass filter 62
Figure 24. Selfoc lens 64
Figure 25. Single mode wavelength division multiplexer 67
Figure 26. Coupling ratio of a 1300/1550 nm single mode wavelength division multiplexer 72
Figure 27. Loss through a 1300/1550 nm single mode WDM 73

Figure 28. $V*d^2(Vb)/dV^2$ as a function of V 78

Figure 29. Proposed datalink 82

Figure 30. Loss through a 1200/1300 nm single mode WDM 89

Figure 31. Total crosstalk at the distribution center . 92

Figure 32. Spectral output of a 1200 nm LED coupled to a 9/125 μm fiber 94

Figure 33. Total crosstalk at the residence 95

1.0 INTRODUCTION

In this information age of ours, communication plays a very important role. Man is constantly striving for a more efficient and faster way of communicating. Fiber optics lends itself as a very agreeable solution since optical fibers have extremely low loss over long distance. They also exhibit an outstandingly large bandwidth and information capacity. They are also very efficient in their small size, light weight and relatively low cost. Fiber optics has already found its way into long-haul communication, local area networks, military applications, sensors, medicine, avionics, industrial control and space exploration.

The constant need for an increasing bandwidth has led designers to enhance the performance of sources and detectors, but since optical fibers have an inherent high bandwidth it makes it a relatively easy solution for the

user to multiplex different optical signals with different wavelengths onto one fiber and thus increasing the information capacity. Wavelength divison multiplexing (WDM) enables us to take full advantage of the optical communication spectrum that extends from 750 nm to 1600 nm over the three main optical windows, the first being at 800 nm, the second being at 1300 nm, and the third being at 1550 nm.

Both bidirectional and unidirectional wavelength division multiplexing have been proven and used in the past few years for point-to-point communication. Bidirectional communication is usually used to communicate with a remote source.

There are two different types of wavelength divison multiplexing in fiber optics [14]. Interwindow wavelength division multiplexing operates with signal channels around 850 and 1300 nm or 1300 and 1550 nm. The attenuation and the bandwidth properties of the optical fiber change over the different communication windows, so this type of communication is suitable for special applications involving dissimilar bit rates.

The second type of wavelength divison multiplexing is intrawindow wavelength division mutliplexing. The signal combination is performed within one of the three optical communication windows. For example, signals are multiplexed in the 800 nm range, at 820, 850 and 880 nm or in the 1300 nm range at 1280, 1300 and 1320 nm. The attenuation and bandwidth are very similar for all signals, but the closer wavelength spacing makes crosstalk and isolation somehow a problem for achieving high speed communication.

Wavelength divison multiplexing in the optical domain has dramatic advantages to mutliplexing in the electronic domain since the optical fiber has a much larger bandwidth [14]. An underground optical cable can be kept untouched while sources and detectors are added at either end of the point-to-point link. A few optical components like WDM's which are usually not expensive and rather simple to implement can be easily added to the already existing fiber optic link.

The following discussion covers an overview of the basic concepts of fiber optics and wavelength division multiplexing system design that incorporates the analysis of the loss budget, crosstalk and bandwidth.

It is going to go into detail when it comes to the operating concepts of the wavelength division multiplexers in both the single mode and the multimode cases, and is going to provide precise experimental data that is crucial to the design of WDM links. The document is concluded with the design of a 20 km bidirectional WDM link.

2.0 BASIC PRINCIPLES

This chapter covers few basic principles of fiber optics. The theory discussed is necessary for our future analysis of couplers and wavelength division multiplexers. Optical fibers are dielectric waveguides capable of guiding and trapping electromagnetic radiation at optical frequencies and transmitting them over a long distance with very low attenuation.

There are basically two approaches to explain the light guidance inside optical fibers. The first approach is based on the fact that the optical wavelength of the transmitted light is very small as compared to the objects the light encounters. The ray analysis of light considers the phenomenon of light transmission as being a succession of plane waves with constant phase known as wavefronts with a separation between any two wavefronts being the wavelength λ.

The propagation of light and the flow of energy are depicted by a ray which is perpendicular to the plane of incidence. Even though the ray tracing method is fairly ambiguous and rather loosely defined because of the restriction on the light to be a perfect plane wave, it provides us with a very intuitive way of analyzing the propagation of light. It is very helpful when considering reflection and refraction at a dielectric interface.

The second approach for studying the propagation of light in a dielectric waveguide is based on solving Maxwell's equations and the boundary conditions. It is a fairly involved method, but it presents us with a more rigorous explanation of the mode propagation phenomena and mode coupling.

Optical fibers are manufactured with a core and a cladding, with the core having an index of refraction larger than that of the cladding. Two types of fiber configurations are available. The first type is the step index fiber where the core has a constant value, and at the core cladding interface the index of refraction abruptly decreases to the level of the index of refraction of the cladding.

The second kind of optical fiber configuration is the graded index fiber. The index of refraction of the core in that fiber (Figure 1), is maximum on the axis and decreases gradually throughout the core until it reaches the cladding. Graded index fibers are used in a multimode regime since they reduce intermodal dispersion, and make the bandwidth much larger than multimode fibers with step index cores.

The refractive index of a dielectric medium plays the most important role in the guidance properties of optical fibers. The index of refraction of a dielectric medium is defined by the ratio of the speed of light in vacuum over the speed of light in the medium. A very important law in fiber optics is Snell's Law for refraction at a dielectric interface. Using the ray tracing method of light, rays are guided in the core of the fiber by successive total internal reflections as shown in Figure 2 [5].

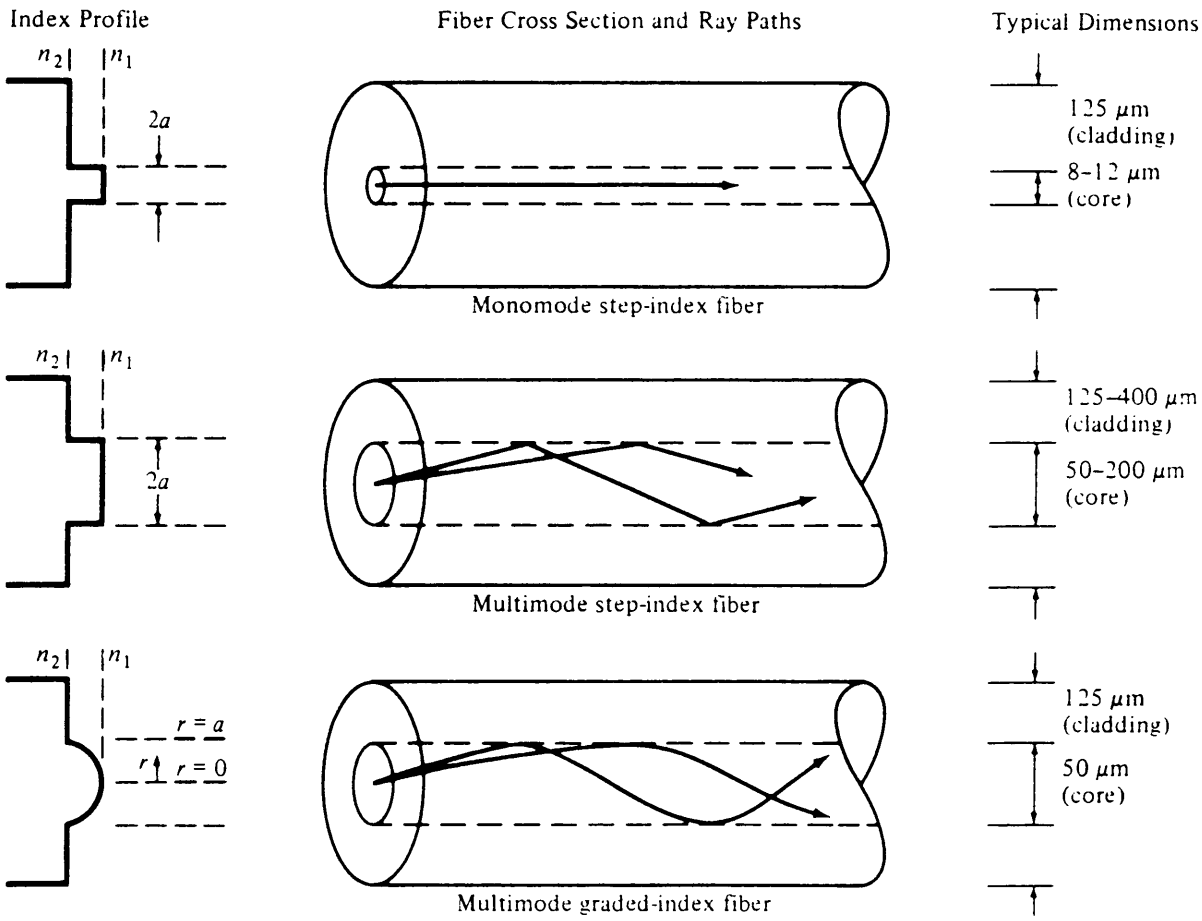

Figure 1

Step index and graded index optical fibers [12].

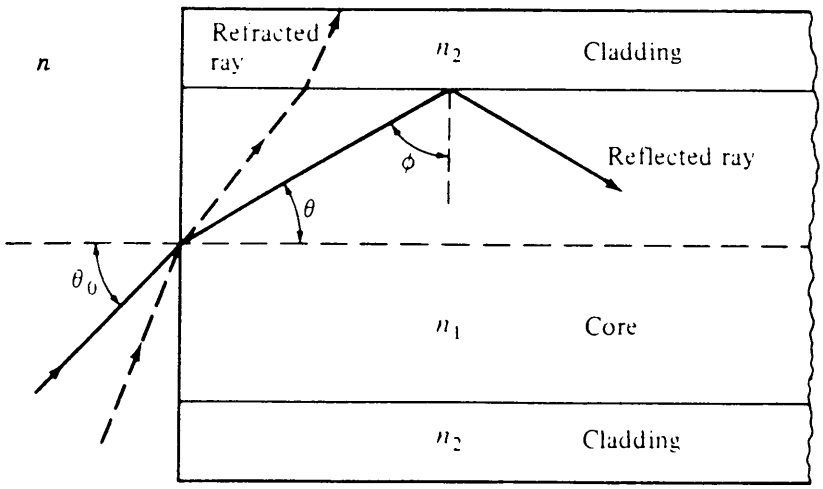

Figure 2

Total internal reflection and numerical aperture [12].

Another important parameter that needs to be defined is the numerical aperture, NA, of the fiber. The numerical aperture for a step index fiber is defined by the sine of half the maximum acceptance angle of the fiber (Figure 2).

$$NA = n \sin \theta_{0,max} = \sqrt{n_1^2 - n_2^2} \approx n_1 \sqrt{2\Delta} \qquad (2\text{-}1)$$

The index difference Δ is given by:

$$\Delta = \frac{n_1^2 - n_2^2}{2\, n_1^2} \qquad (2\text{-}2)$$

and since $n_1 \approx n_2$

$$n_2 \approx n_1 (1 - \Delta) \qquad (2\text{-}3)$$

In multimode fibers, since the core radius is relatively larger than the wavelength of the transmitted light, we can approximate the guided light as local plane waves that are reflected at the core-cladding interface. It is then feasible to use the ray optics interpretation. The index of refraction n(r) of a graded index fiber is given by:

$$n(r) = \begin{cases} n_1 \left[1 - 2\triangle (r/a)^{\alpha} \right]^{\frac{1}{2}} & 0 \leq r \leq a \\ n_2 & r \geq a \end{cases} \qquad (2\text{-}4)$$

α defines the shape of the index profile.

The NA of a graded index fiber is given by:

$$NA(r) = \begin{cases} \left[n^2(r) - n_2^2 \right]^{\frac{1}{2}} & r \leq a \\ 0 & r > a \end{cases} \qquad (2\text{-}5)$$

Graded index fibers have their core composed of different layers of a doped core, and as the rays move away from the central axis they encounter layers of decreasing index of refraction. We can intuitively consider the optical rays being refracted by the different layers of the core, and they eventually trace a sinusoidal path along the core. We are going to discuss the propagation of rays in a lens like medium in a fairly detailed manner when we come to the discussion of Selfoc lenses. We noticed that higher order modes (rays) are reflected by the core material at a

distance farther away from the axis than lower order modes. This phenomenon reduces intermodal dispersion by making the group velocity of high order modes equal to that of low order modes.

When light is travelling inside the core of an optical fiber, it is considered an elecgromagnetic wave. To obtain a more detailed description of the propagation of light in optical fibers, we have to solve Maxwell's equations in a linear, isotropic dielectric without currents or free charges, and have our solution meet all boundary conditions [6],[9],[12].

An optical fiber supports a finite number of discrete guided modes and an infinite number of continuum of radiation modes that are not trapped in the core, but are still solutions to Maxwell's equations and satisfy boundary conditions. A mode will remain guided if its propagation constant β satisfies the following condition:

$$n_2 < \beta/k \leq n_1 \qquad (2\text{-}6)$$

where $k = 2\pi/\lambda$ (2-7)

λ is the free space wavelength

Cutoff occurs when $\beta = n_2 k$, and an important parameter connected with cutoff is the V number.

$$V = ka \sqrt{n_1^2 - n_2^2} \qquad (2\text{-}8)$$

Cladding modes that are guided by the cladding and jacket interface are supressed by the lossy coating, and are scattered out of the fiber after travelling a short distance.

3.0 BIDIRECTIONAL WDM DATALINK

Figure 3 shows the bidirectional system that we plan to analyze and design. Such a system is used for point-to-point communication over one fiber. It enables the user to communicate with a remote location. Signals on channel with wavelength λ_1 may carry control information, and the return channel with wavelength λ_2 would send back a continuous stream of data, for example. Two very important design considerations have to be established first. Number one, the distance between the two locations and number two, the data rate required.

The proposed system consists of a source with peak emission wavelength λ_1 connected to a wavelength division multiplexing device that launches the λ_1 signal onto the link fiber. The same wavelength division multiplexing device directs the signal with wavelength λ_2 to the detector fiber, and provides enough isolation between the

source and the detector in order to make the communication link feasible. The wavelength division demultiplexing operation is performed by a similar device at the other end of the link. At this point, we have the choice of two technologies. The single mode and multimode fiber optic communication.

We also have three choices for the wavelength λ_1 and λ_2. We can use interwindow wavelength division multiplexing by choosing one wavelength in the 800 nm range and the other in the 1300 nm range for example. We can use intrawindow wavelength division multiplexing and choose both wavelengths to be in the 800 nm window.

Choosing the wavelength is dependent on the result of the power budget, bandwidth budget and total cost. The cost of components whether emitters or detectors is relatively low in the 800 nm window. The detectors are made with silicon, and the silicon technology is mature, and has low material cost. Sources and detectors in the 1300 and 1500 nm windows are still rather expensive. They use GaAs technology which is still new and expensive. The design of WDM link requires a thorough understanding of optical sources.

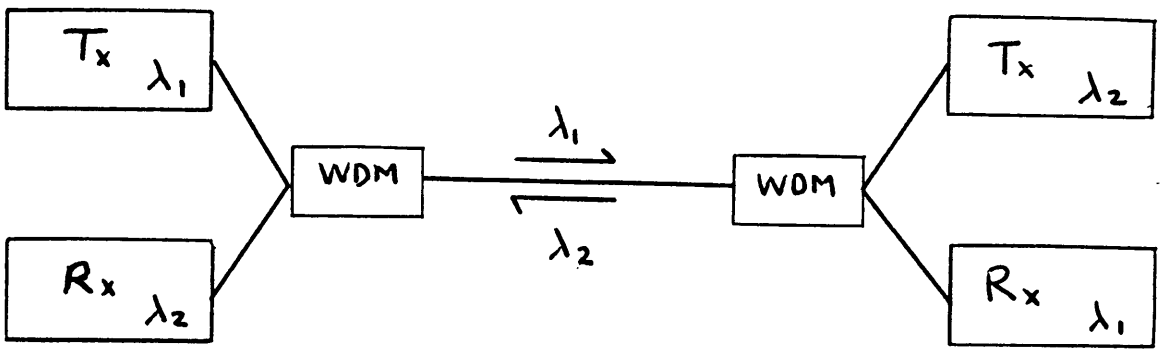

Figure 3

Bidirectional WDM datalink.

4.0 FIBEROPTIC SOURCES

Fiber optic systems utilize two categories of sources. Light emitting diodes (LED's) and laser diodes. Lasers are used in long distance communication where high power and large bandwidths are a necessity. LED's are used in applications requiring transmission distances up to several kilometers and speeds up to about 100 Mb/sec. LED's are in general less expensive than lasers. Their emitted power has a smaller dependence on temperature variations. They are more reliable over time and they require a simpler drive circuit. The disadvantages of LED's are low power, low modulation speed, incoherence and wide spectral width.

4.1 PRINCIPLES OF OPERATION OF AN LED

An LED is essentially a p-n junction that under the conditions of forward bias spontaneously emits light. When an LED is forward biased, minority carriers cross the junction and recombine. During the recombination process every electron-hole pair gives rise to a photon with energy roughly equal to the band gap energy of the material used. During the recombination process, both energy and momentum have to be conserved.

Semiconductor materials with indirect band gaps require the emission of a phonon and a photon during recombination. The phonon which could be translated into crystal lattice vibration is responsible for the conservation of momentum. The photon with energy equal to hc/λ is responsible for the conservation of energy, where h is Planck's constant, c is the speed of light in vacuum, and λ is the wavelength.

A more efficient radiative recombination, where only photons are emitted, occurs in direct band gap materials where the most probable recombination process occurs between electrons and holes with the same momentum value.

Figure 4 shows the recombination process in (a) direct band gap semiconductors and (b) indirect band gap semiconductors. The majority of infrared LED's used in fiber optics are constructed with direct band gap semiconductors because of the higher intrinsic emission efficiency.

None of the normal single element semiconductors are direct band gap materials, but many binary III-V compounds are. These compounds are made of group III elements (Al, Ga, In) and group V elements (P, As, Sb). GaAs diodes emit peak power at a wavelength around 940 nm, which is not a desirable wavelength for fiber optics because of the high attenuation in glass fibers. By adding Al to form GaAlAs, the diode yields maximum emission at a wavelength between 800 and 900 nm. By changing the mole fraction of Al in the compound, we can specify the exact wavelength of peak emission.

Since the wavelength of minimum dispersion in optical fibers is around 1300 nm, and the wavelength of minimum attenuation is at 1550 nm, optimized communication links require sources at these long wavelengths. LED's can be made with the quarternary alloy InGaAsP to emit optical power at any wavelength between 1000 and 1700 nm [7].

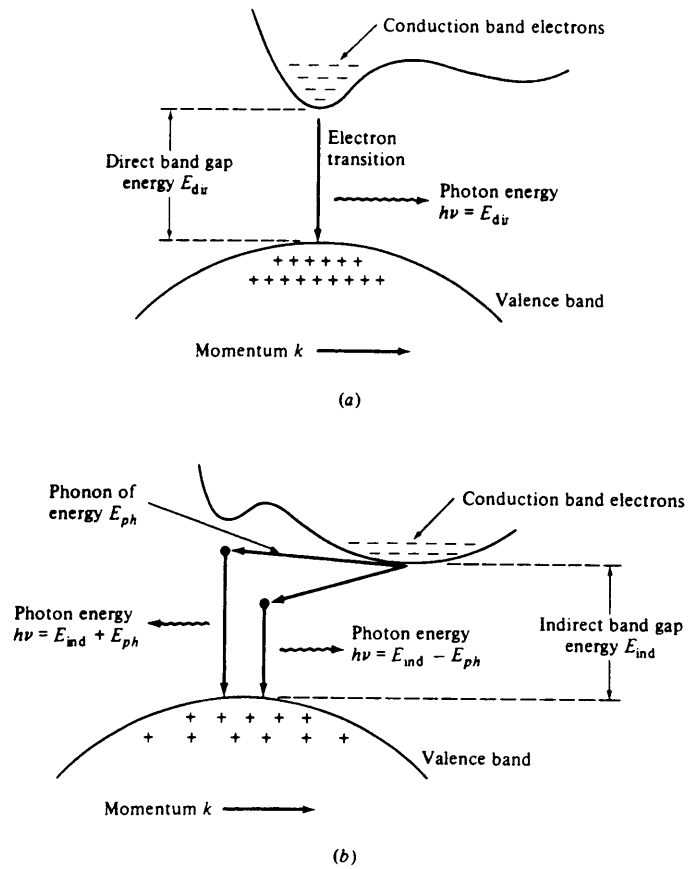

Figure 4

Electron recombination for

(a) direct band gap material and

(b) indirect band gap material [12]

The peak emission wavelength is related to the band gap energy E_g by the following equation:

$$\lambda\ (\mu m) = \frac{h\ c}{E_g} = \frac{1.240}{E_g\ (eV)} \qquad (4\text{-}1)$$

since the emitted photon has an energy equal to E_g, caused by the recombination of an electron and a hole across the energy band gap.

There exists a number of energy sub-levels in the region of the conduction and valence bands of the semiconductor that can support additonal recombinations. This results in emitted photons with wavelengths in the neighborhood of the wavelength of peak emission. Spontaneous photonic emission is sustained as long as energy and momentum are conserved during the recombination process betwen two energy levels. The output spectrum of an LED is therefore broad as compared to that of a laser diode. The spectral width of an LED which is defined by the wavelength spread, $\triangle \lambda$, between the halfpower points, is typically in the range between 30 and 120 nm.

4.1.1 EXPERIMENTAL MEASUREMENTS OF THE LED SPECTRUM

The system used to measure the LED spectral output is shown in Figure 5. It is a highly sensitive and dynamic measurement system with a slit width of 5 nm. This basically means that the system takes a reading every 5 nm interval. The output of the LED is modulated at a frequency of 200 Hz, and the lock-in amplifier is configured to measure the current at that frequency. The output spectrum is shown in Figure 6. We notice that the measurements are in agreement with the formula for the LED spectrum $\Gamma(\lambda)$ given by Nosu [3].

$$\Gamma(\lambda) = \frac{1}{1 + \left[\frac{2(\lambda - \lambda_0)}{\Delta\lambda}\right]^3} \qquad (4\text{-}2)$$

where λ_0 and $\Delta\lambda$ are the center wavelength and the full width half maximum (FWHM) spectral width respectively.

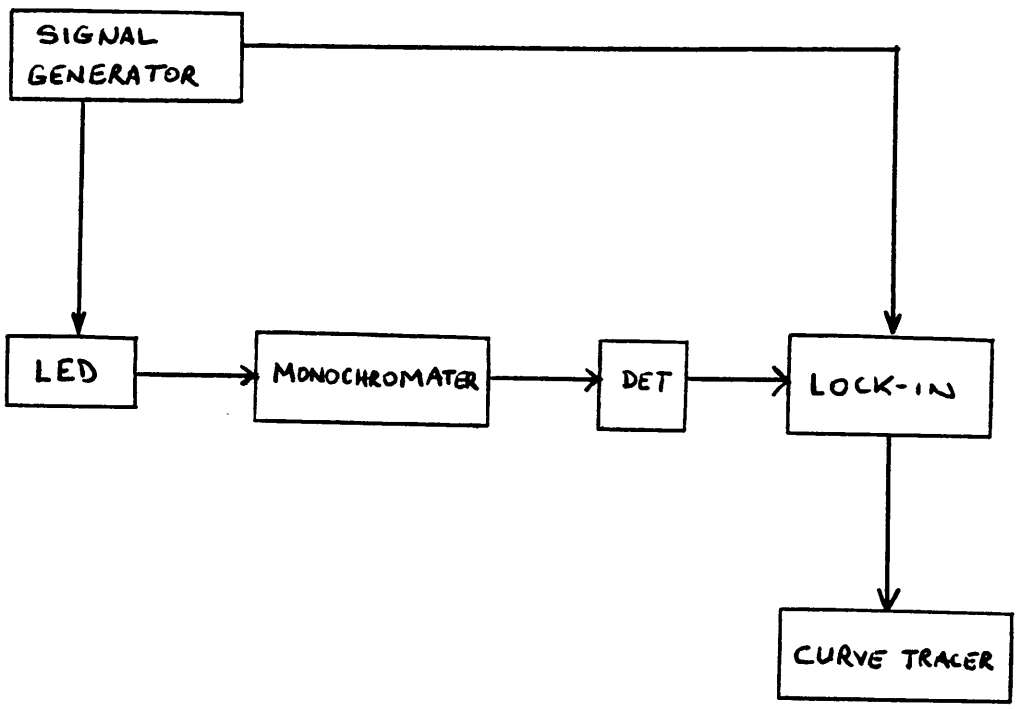

Figure 5

Output spectrum measurement system.

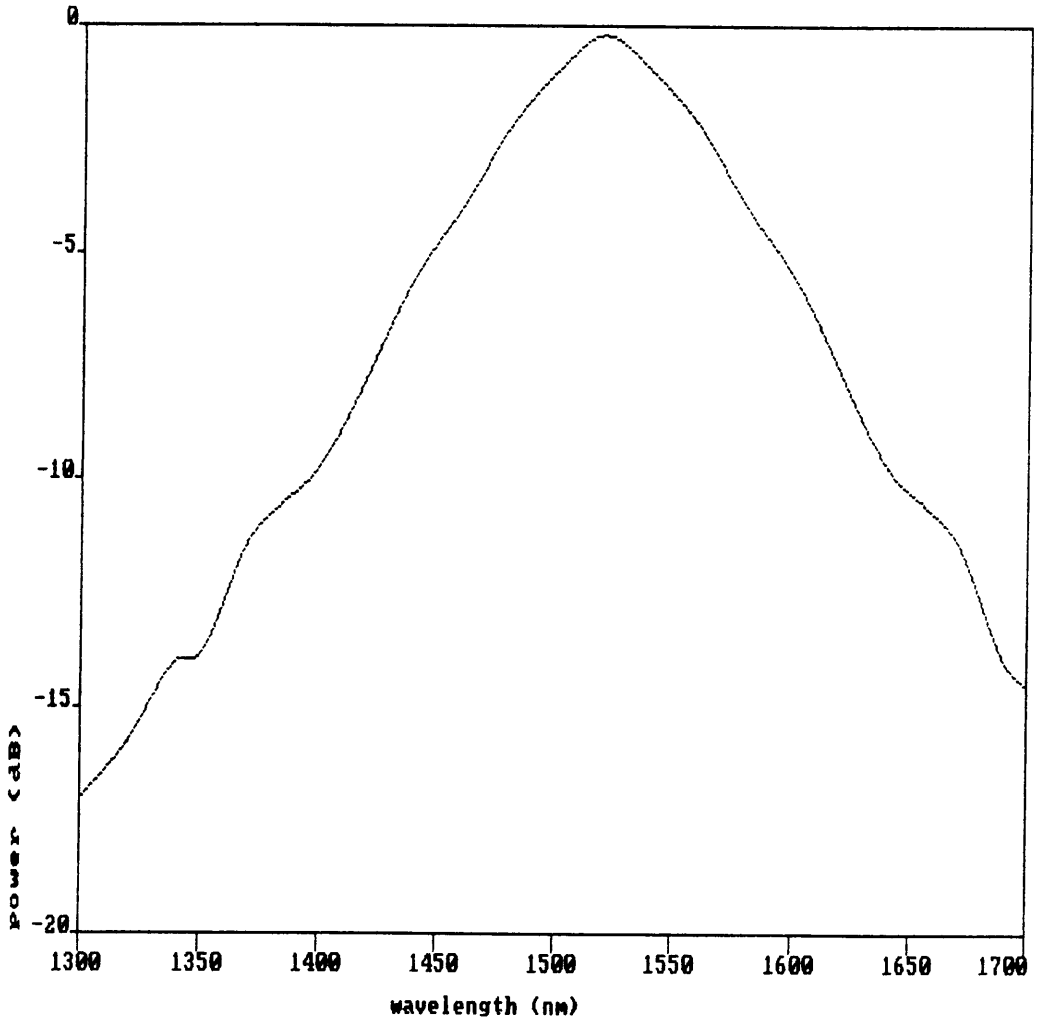

Figure 6

Output spectrum of a 1520 nm LED

which is coupled to a 9/125 μm fiber.

4.1.2 DESIGN CONFIGURATIONS

LED's are divided into two main configurations: surface emitters and edge emitters. Surface emitters are simple to construct, and they can be a planar homojunction which is a p-n junction formed by doping a single material or a heterojunction. A heterojunction LED has multiple junctions formed of materials with different doping levels. A schematic of a planar double heterojunction AlGaAs LED is shown in Figure 7.

The purpose of the heterostructure is to confine carriers to a small area where recombination occurs. The smaller emitting area of a heterojunction LED makes coupling the optical power from the LED to the fiber core much more efficient. The band gap differences of the adjacent layers in a heterostructure configuration confine the charge carriers into the narrow active region. The resulting output from a surface emitter is Lambertian, which means that the intensity of the emitted power is proportional to the cosine of the angle with the normal to the emitting surface.

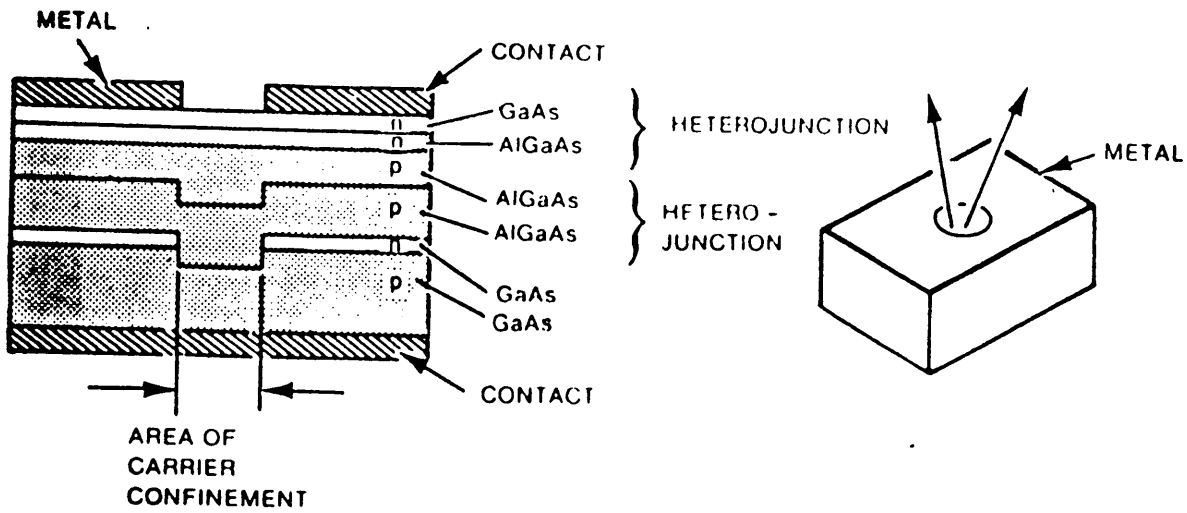

Figure 7

Planar double heterojunction LED

However, increasing carrier confinement to achieve higher efficiency and higher radiance has its limits. The current density through a narrow active region becomes large, and causes an increase in the junction temperature which could eventually lead to failure. There are some basic parameters which influence the performance of a device, and they are:

* Self absorption; absorption in the active region and around it.

* Recombination at the secondary heterojunction interfaces.

* Doping concentration of the active layer.

* Rated injection carrier density required to reach optimum output power.

* Dimensions of the active region.

The second kind of LED is referred to as an edge emitter. A similar heterojunction structure is used, but rather than having the active region as a disc, it is configured into a stripe (Figure 8).

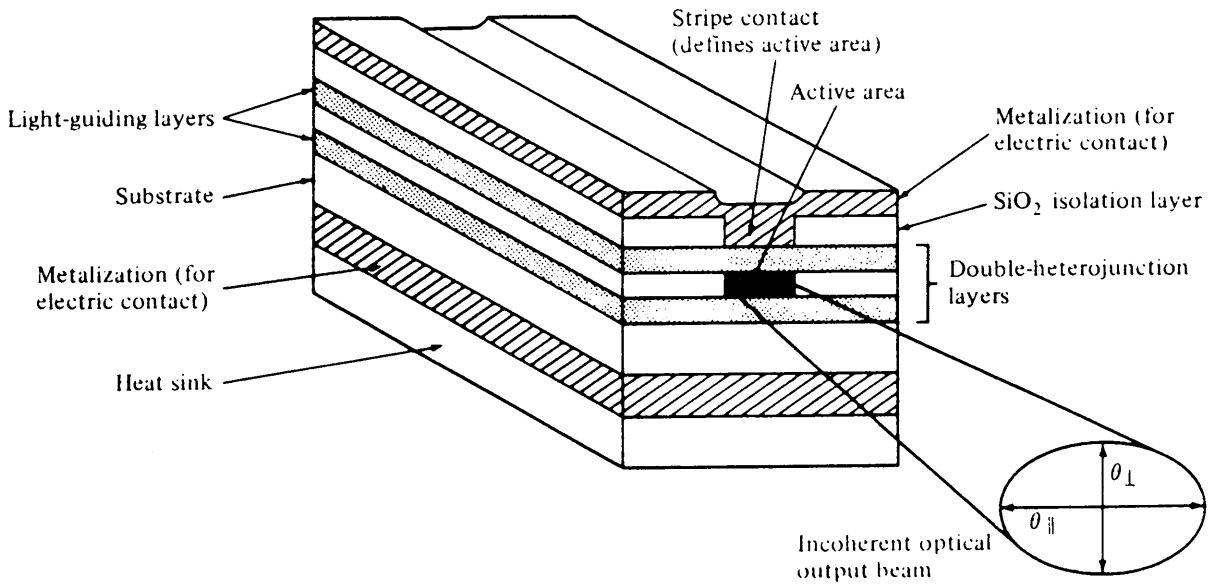

Figure 8

Edge emitting LED [12]

The use of a metal and oxide layer makes the stripe feasible by confining the photons longitudinally. Both optical and carrier confinement is reached by having adjacent layers with different indices of refraction and different energy band gaps. The special waveguide effect in an edge emitter produces a directional output beam which can be coupled into optical fibers more easily. Edge emitting LED's are more stable with respect to temperature than surface emitters because of the large active area with relatively low carrier density flowing through it. Yet a large active region, yields a large device capacitance which makes edge emitters relatively slower than surface emitters.

4.1.3 OPERATING PARAMETERS AND CHARACTERISTICS

A list of the operating parameters of an LED according to the order of importance to a fiber optics design engineer is as follows:

* wavelength of peak emission
* output power
* speed and bandwidth
* spectral width
* reliability

The wavelength of peak emission and the output power are selected following a power budget analysis of the fiber optic system. The wavelength of transmission has to fall in the range of minimum attenuation of the optical fiber.

A typical plot of the output power versus the drive current for an LED is shown in Figure 9. The speed and bandwidth of the LED depend on the internal quantum efficiency, junction space charge capacitance and diffusion capacitance. The internal quantum efficiency in the active region is the fraction of electron-hole pairs that recombine radiatively over the total number of electron-hole pairs that recombine. We saw earlier that not all recombinations result in a photonic emission, some electron-hole recombinations produce phonons, and eventually cause heating of the active region.

If R_r is the rate of radiative recombination and R_{nr} is the rate of nonradiative recombination, then the internal quantum efficiency, τ_o, is given by:

$$\tau_o = \frac{R_r}{R_r + R_{nr}} \qquad (4\text{-}3)$$

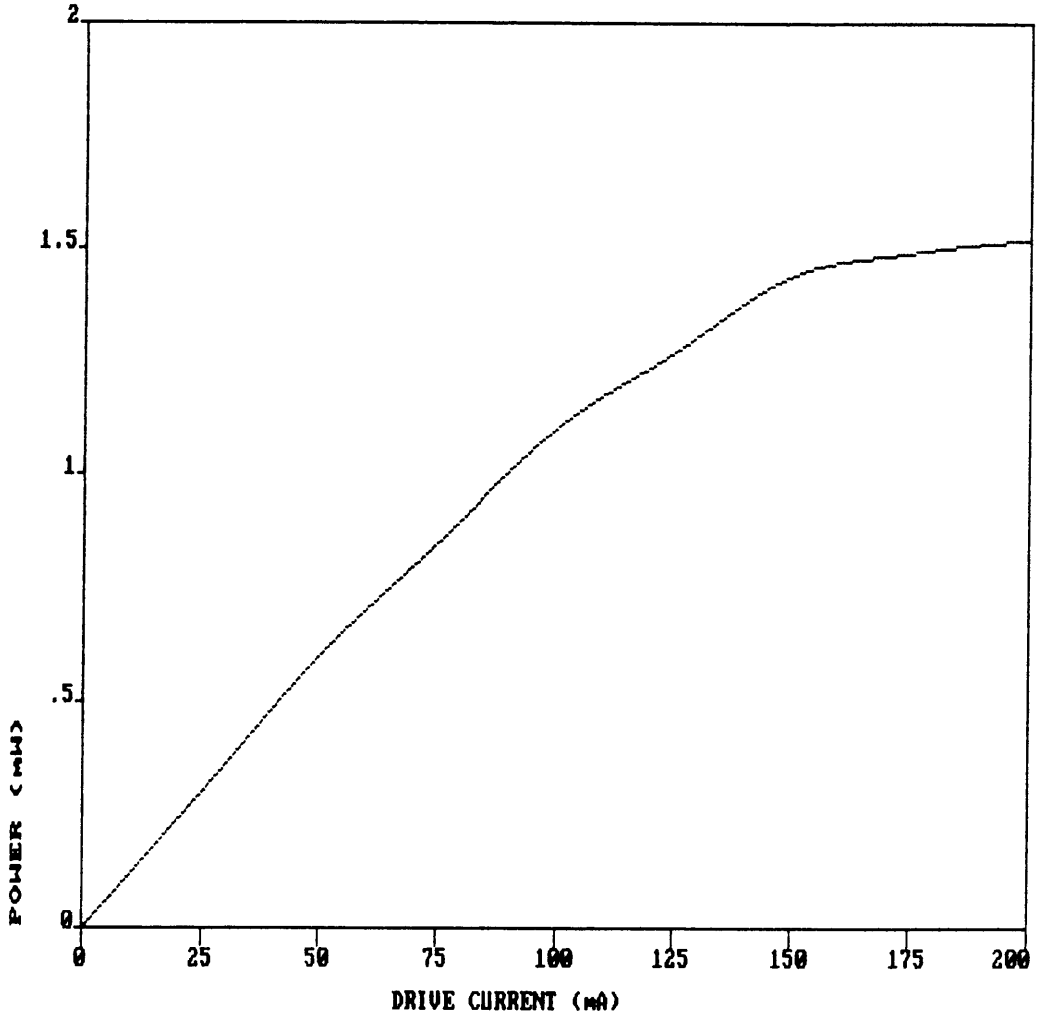

Figure 9

LED output power versus drive current.

Self absorption also contributes to the reduction of the overall efficiency and bulk lifetime. The internal absorption is more severe in p-type materials than in n-type materials. The speed and bandwidth of an LED are limited by the diffusion capacitance of the active region. The power of the optical signal varies with the frequency of modulation, w, in the following manner:

$$I(w) = \frac{I_0}{\left[1 + (w\, t_{eff})^2 \right]^{-\frac{1}{2}}} \qquad (4\text{-}4)$$

The 3-dB modulation bandwidth is therefore:

$$B = 1/t_{eff} \qquad (4\text{-}5)$$

Another important characteristic of the LED is its spectral width which plays a very important role in crosstalk analysis of closely spaced channel on a WDM communication link [8].

The reliability of an LED is much larger than that of a laser. The expected lifetime of an LED is in the excess of 500,000 hours of operation at the nominal drive current.

The materials used for the heterojunction structure as well as the fabrication procedure play a crucial role on the operational lifetime of the chip. The packaging affects the overall lifetime of the device, and we realize in every day experience with LED's that it is rare for a chip to get damaged. Most of the device failures are either the result of the break down of the package or the power coupling mechanisms.

4.1.4 EXPERIMENTAL MEASUREMENTS

The following measurements were performed on an edge emitting LED. The barrier height is calculated to be in the order of 0.6 to 0.7 Volts. The series resistance of the bulk semiconductor is measured at 100 mA forward bias, and it has a value in the range from 3 to 4 Ohms. The rise and fall times of a 1300 nm LED after it has been packaged are shown in Figure 10. Both the rise and the fall time depend on the magnitude of the bias current. The relationship is shown in Figure 11.

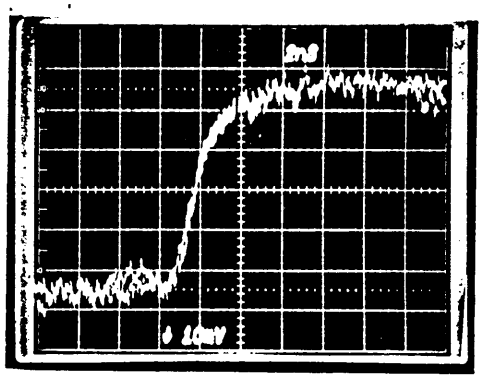

t_{rise}

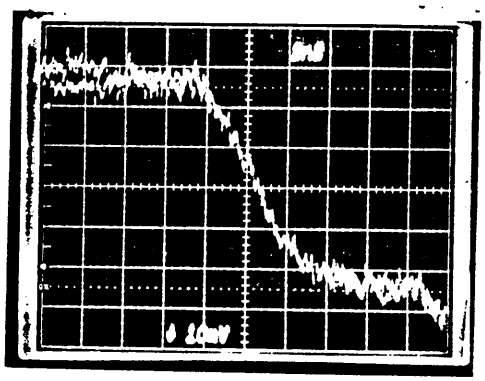

t_{fall}

Figure 10

Rise and fall time of

edge emitting LED.

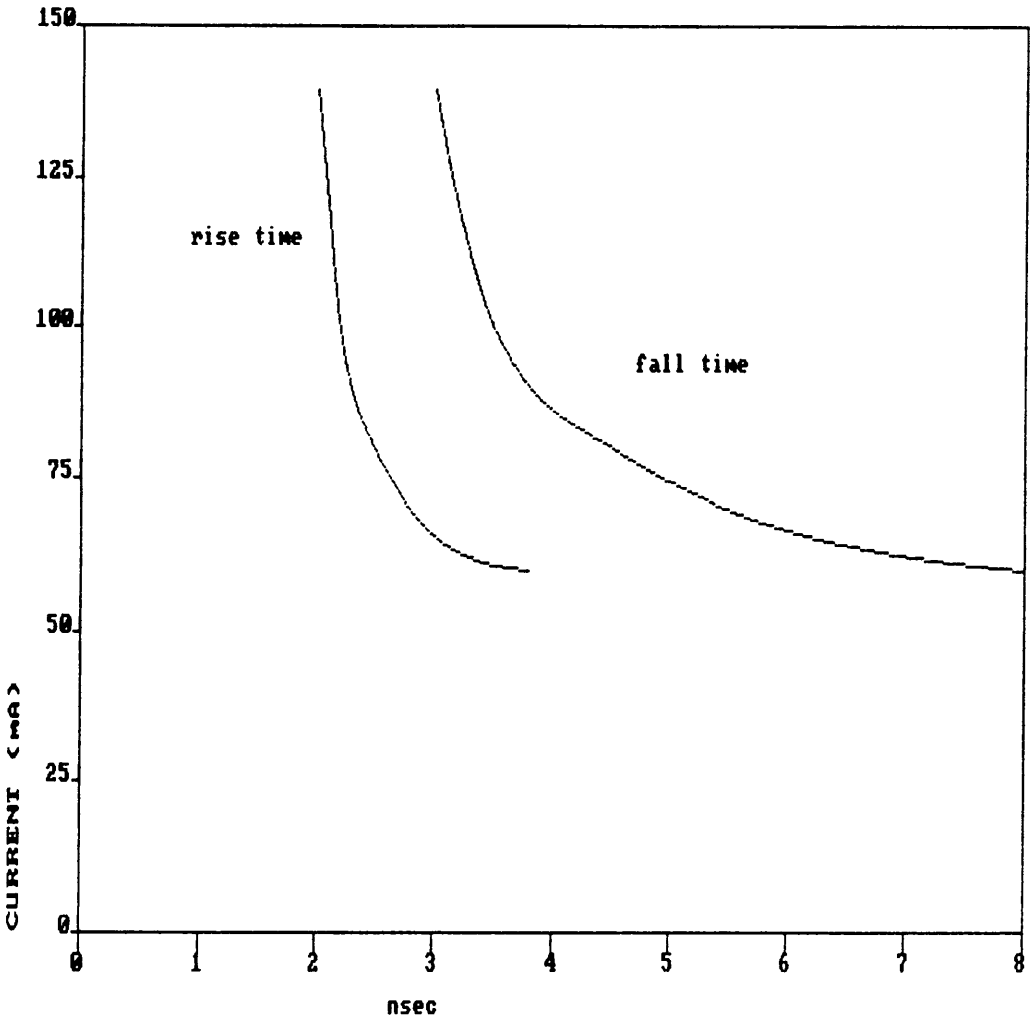

Figure 11

Rise and fall time of an edge emitting LED versus drive current.

4.1.5 TEMPERATURE DEPENDENCE

As the operating temperature of an LED varies , many of its parameters change accordingly. The wavelength of peak emission, the spectral width, the peak output power, all depend on temperature. This dependence is primarily linked to the variation of the energy band gap and the distribution of the energy levels at the top of the valence band and at the bottom of the conduction band.

A plot of the spectral response of a 1300 nm edge emitting LED at different temperatures is shown in Figure 12. Table 1 lists the exact values of the peak wavelength and the spectral width as a function of temperature. LED's experience high radiance at low temperature and saturation at high temperatures.

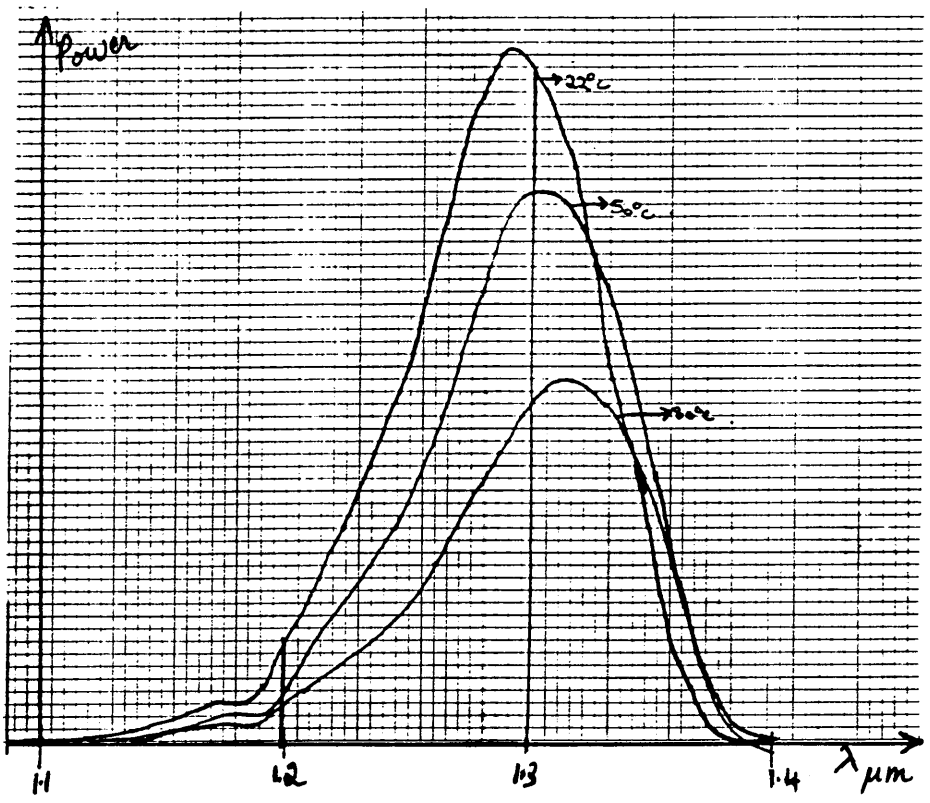

Figure 12

Output spectrum of an edge emitting

LED with respect to temperature variations.

Temperature (°C)	Peak λ (nm)	FWHM (nm)
-25	1264	82
0	1280	88
25	1290	90
50	1302	92
80	1316	96

Table 1

Center wavelength and FWHM spectral width of an EELED versus temperature.

4.2 LASER DIODES

With the performance of the LED's in mind we can now analyze the second important source in fiber optics which is lasers. The majority of lasers used for fiber optic communication are designed with the Fabry-Perot resonator cavity with optical gain. An example of the structure of the laser is shown in Figure 13. We noticed the heterostructure design of the laser along with an optical cavity which provides amplification.

During normal operation, the laser chip is forward biased which causes spontaneous emission in the active area. Photonic absorption in the active area takes place, and the presence of the gavity with optical gain causes stimulated emissions of photons with specific energy. Stimulated emissions take place at a rate that exceeds absorption when the state known as population inversion occurs. Population inversion is when the population of the excited states is greater than that of the ground state.

Lasers are threshold devices which means that the lasing activity occurs when a certain level of current is reached.

Mass Transport—Buried Heterojunction Diode
Laser Structure

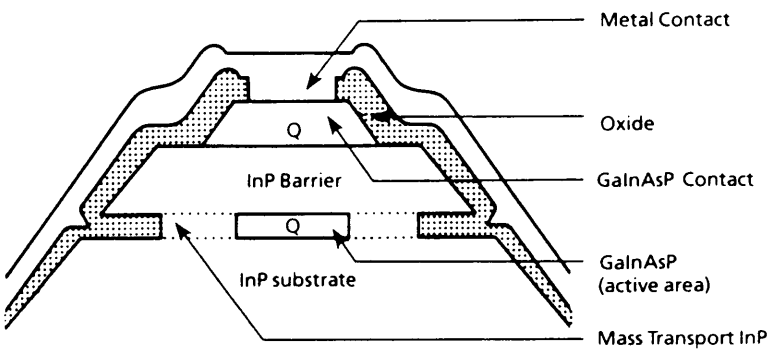

Figure 13

Configuration of a laser diode.

Below that level, spontaneous emission occurs and the performance of the chip is similar to that of an edge emitting LED. At threshold, population inversion takes place and the lasing activity start. Beyond threshold, the output of the laser beam is highly monochromatic and coherent. A plot of the output power versus the input current is showed in Figure 14. We notice the dramatic change in the slope of the curve beyond threshold.

The laser cavity is fabricated by forming a very narrow stripe for the active area, and depositing a partially reflecting dielectric mirror on both facets. The cavity exhibits optical gain due to stimulated emissions in the active area and successive reflections from its sides. Just like LED's, lasers in the 800 nm window are fabricated with GaAlAs while lasers in the 1300 and 1550 nm windows are fabricated using the alloy InGaAsP.

The lasing in the resonator cavity provides an output beam with a fairly collimated pattern. The full width half maximum spectral width into an optical fiber is typically 1 to 5 nm, and the power coupled into a single mode (9/125 μm) fiber is in the order of 1 mW.

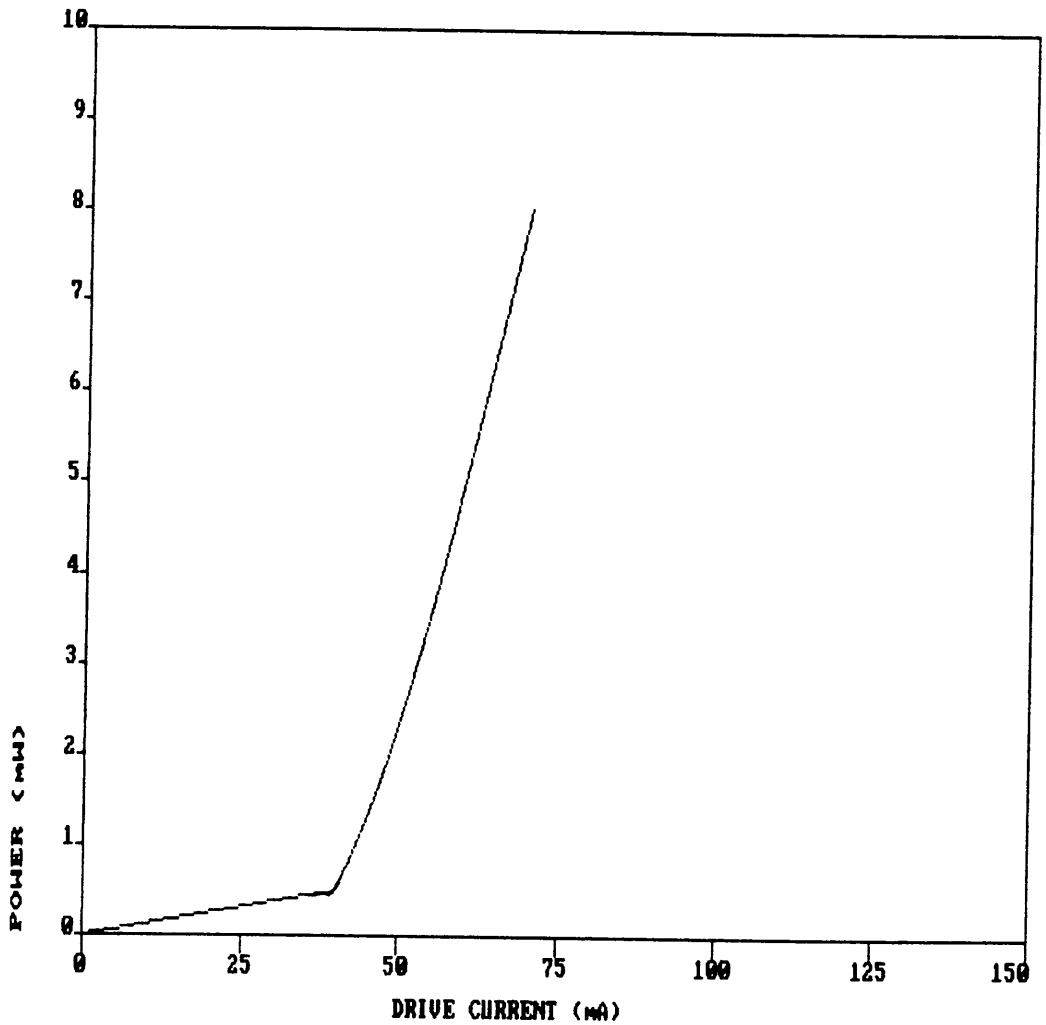

Figure 14

Output power versus drive current for a laser diode.

The response time is usually less than 1 nsec, which makes high speed modulation possible. Lasers are capable of transmitting at data rates up to 1 Giga bit per second, and distributed feedback lasers which use a grating to establish feedback in the cavity are able to achieve transmission speeds up to 20 Gb/sec and more.

A typical value of the current at threshold for a Fabry-Perot cavity laser is anywhere from 20 to 50 mA. The rated output power is achieved at about 30 mA above threshold.
An important parameter which defines the quality of a laser is the external differential quantum efficiency. It basically gives us an idea about the slope of the power versus current beyond the threshold. The differential quantum efficiency is given by:

$$\delta = \frac{e}{E_g} \frac{dP}{dI} \qquad (4\text{-}6)$$

where e = electronic charge

E_g = energy gap

P = output power

I = drive current

Lasers are very sensitive to temperature changes. The total output power, the wavelength of peak emission, the threshold current and many other operating parameters change with temperature. This phenomenon is similar to what we observed in the edge emitting LED. The change in the threshold and differential quantum efficiency makes it a tough task for the design engineer to compensate for them with temperature. One of the ways to solve that problem is to mount the laser chip on a thermoelectric device.

4.2.1 THERMOELECTRIC DEVICES

Thermoelectric devices are solid state heat pumps. They are very small in size, and are able to reach temperature differentials of 50 degrees Celcius and more [16]. The cross section of a typical thermoelectric device is shown in Figure 15. Electrons crossing from the P to the N type semiconductor (P-N interface) absorb energy in the form of heat, and jump to a higher energy level. By doing so, they help cooling the surface at that junction. At the N-P junction, electrons move to a lower energy state, and release energy in the form of heat. A DC power source helps the electrons move along the closed circuit.

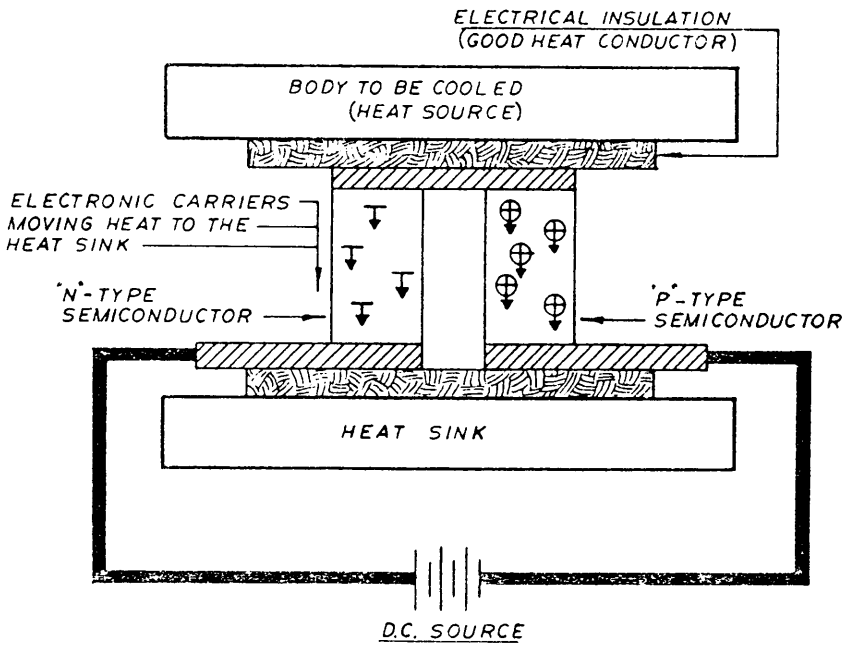

Figure 15

Cross section of a typical thermoelectric cooler. [16]

A heat sink is connected to the N-P interface in order to transfer the heat that was pumped into the environment. Special attention has to ge exercised in designing the heat sink in order to provide adequate thermal path and thermal mass.

The semiconductor material used is primarily Bismuth Telluride, heavily doped to create N and P type semiconductors. Thermoelectric cooling couples are assembled in the form of a module by connecting the junctions in series electrically and in parallel thermally. A typmcal module assembly is shown in Figure 16.

Thermoelectric coolers (TEC) are used to maintain the chip temperature of both lasers and LED's at 25 degrees C when the ambient temperature varies from -30 to +70 degrees C. A typical cooler current at 70 degree C is around 800 mA, while the voltage is typically less than 1.5 volts. The cooler response time is in the order of 10 seconds which is relatively quick. The response time in this case is defined as the time taken by the cooler to change the temperature of the chip from 70 degrees C to 25 degrees C. TEC's are a very important device for lasers that are used in environmentally unstabled surroundings.

Thermoelectric coolers help stabilize the temperature of the chip at 25 degrees C or any other temperature depending on what is optimum for the specific application. By doing so, the performance and parameters of the laser are kept relatively constant. LED's also use thermoelectric coolers in order to prevent the wavelength of peak emission and output power from changing which could be detrimental in a wavelength division multiplexing system with closely spaced wavelengths.

The disadvantages of TEC's are that they tend to consume considerable electrical power, they add to the complexity of laser drive circuits by requiring a temperature controller, and thus increase the cost of the system.

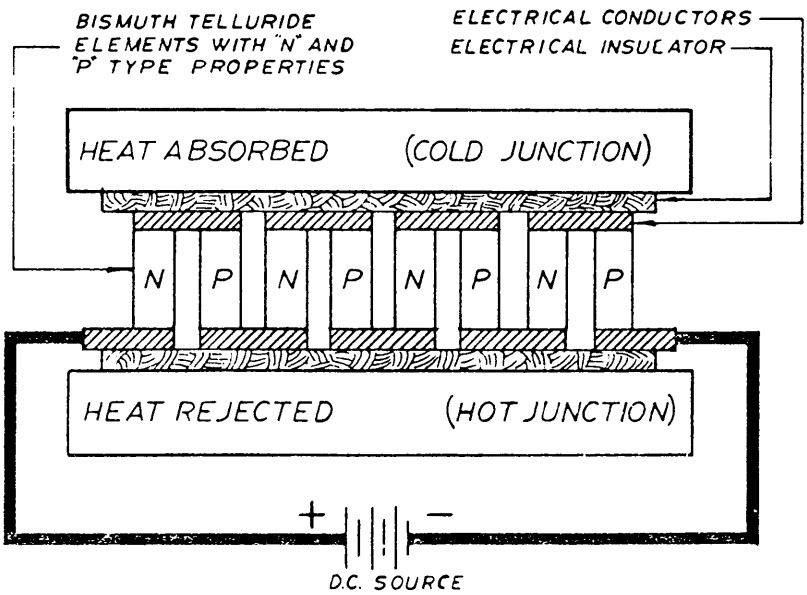

Figure 16

Thermoelectric module assembly. [16]

4.2.2 EXPERIMENTAL RESULTS

Using the measurement set-up of Figure 5, the output spectra of a 1310 and 1290 nm lasers were measured (Figures 17 and 18). Both laser diodes are packaged in a 14 pin dual in line package with TEC, and coupled to a single mode fiber (9/125 μm). This analysis enables us to study the out-of-band emissions of a laser diode which play a major role in the crosstalk of WDM links.

To evaluate the temperature dependence of 1300 nm single mode laser diodes with TEC's, we temperature cycled it from +70 degrees C to -40 degrees C. For an optically stabilized laser, we found that the maximum change in the output power to be 0.5 dB, and the maximum change in bias current to be 0.76 mA. No change in the peak wavelength was detected.

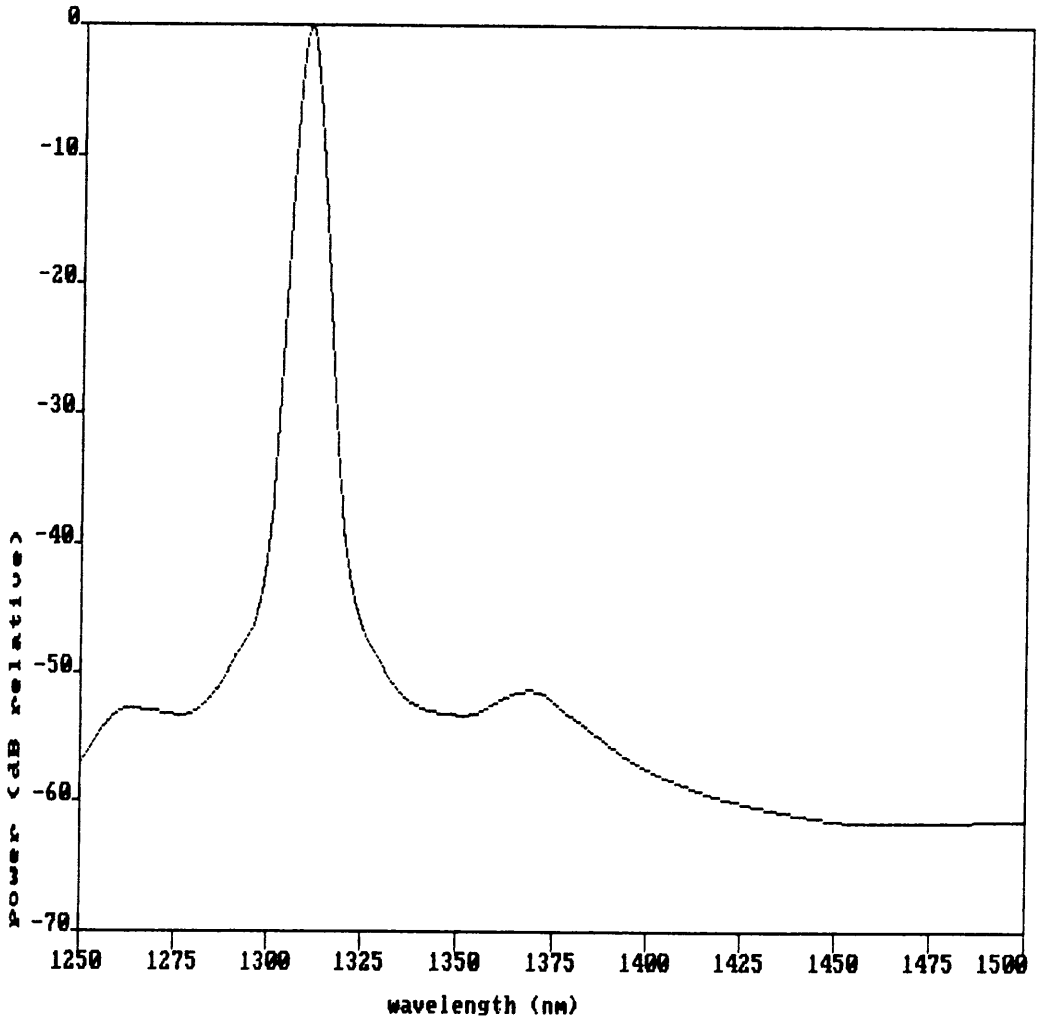

Figure 17

Output spectrum of a 1310 nm laser which is coupled to a 9/125 μm fiber.

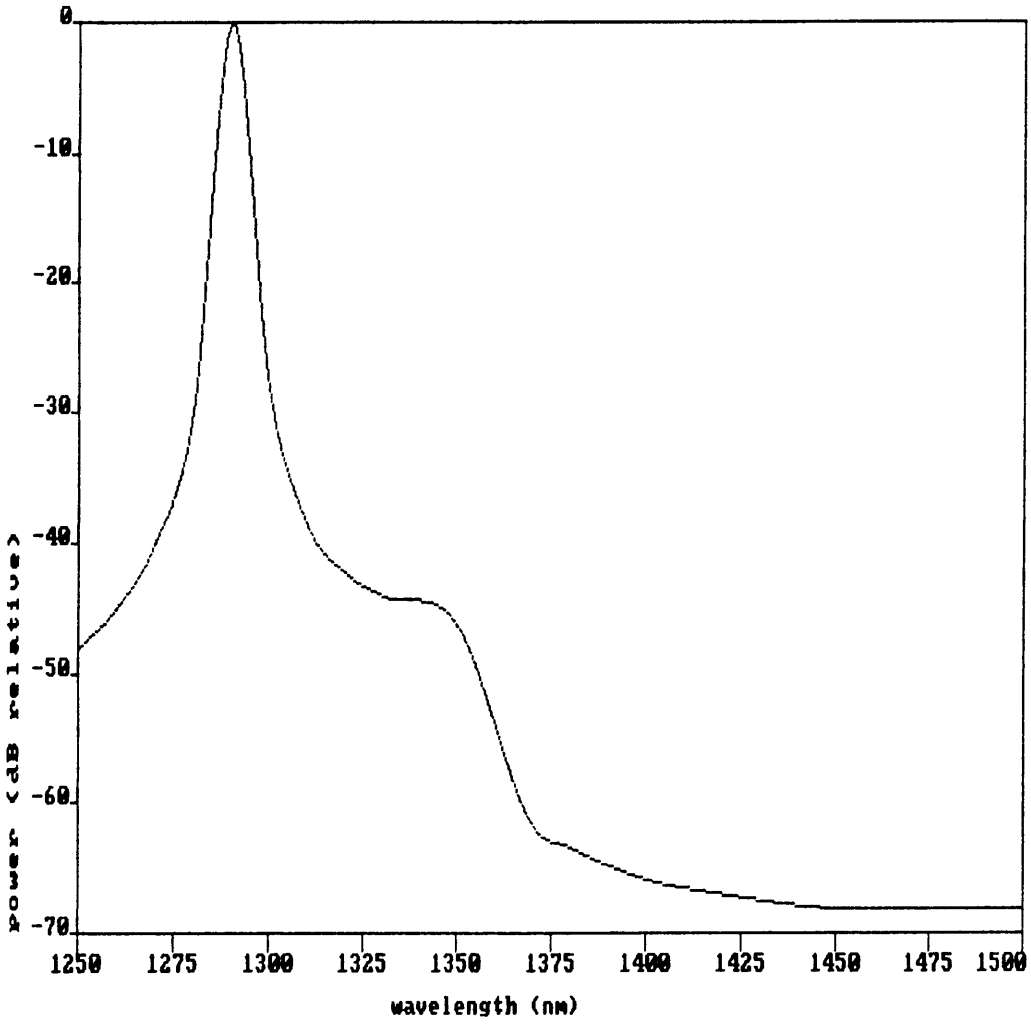

Figure 18

Output spectrum of a 1290 nm laser which is coupled to a 9/125 μm fiber.

5.0 PHOTODETECTORS

The two main types of photodetectors used in fiber optic communication are PIN diodes and Avalanche photodiodes (APD's).

5.1 PIN PHOTODIODES

A typical PIN diode configuration is shown in Figure 19. The P region refers to a P type doped semiconductor. The I is an intrinsic type semiconductor which means it has no doping, and the N region is an N type doped semiconductor. Photons shining on the intrinsic region cause the generation of electron hole pairs. The reverse biaw voltage which is applied to the photodetector creates an electric field which separates the newly generated electrons and holes. The current is then amplified, and thus the detection of incident photons is achieved.

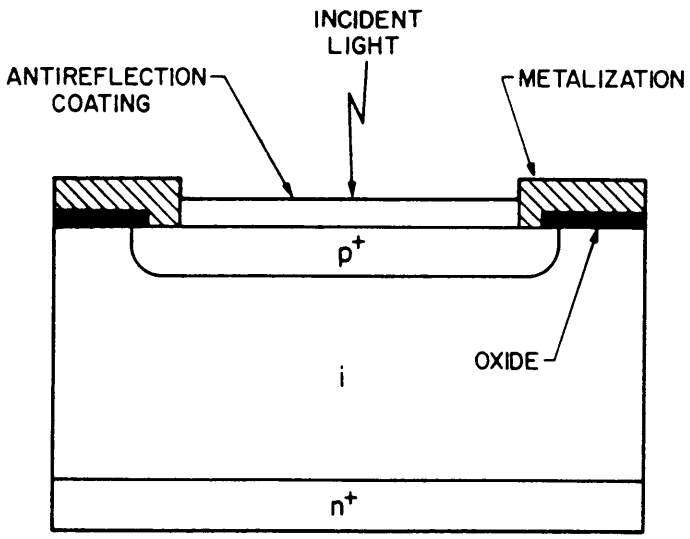

Figure 19

PIN photodiode configuration. [27]

Silicon is the material of choice for low wavelength detection (800 nm). Ge and InGaAs are used for long wavelength detection. The Ge detection spectrum is wider, as it stretches from 800 nm to about 1700 nm. InGaAs detects photons with wavelengths from 1000 nm to about 1800 nm.

An important parameter that specifies the quality of a photodetector is the quantum efficiency, η. The quantum efficiency is defined by the number of electron-hole pairs divided by the number of incident photons. The quantum efficiency is always less than unity because of three main occurances. The incident light is sometimes reflected at the interface between the surrounding medium and the detector surface. The optical reflection does not allow the detection of any of these photons. The second case is when light and photons pass through the I type region without being absorbed and without generating electron-hole pairs. This is usually the case when the absorption occurs in the N type region. The third case is when the electron-hole pairs recombine to form and emit a photon. This recombination rate reduces the quantum efficiency of the photodetector. A parameter that is related to the quantum efficiency ,and can be easily measured is the responsivity, R (Figure 20).

$$R = \tau \frac{\lambda q}{h c} \qquad (5\text{-}1)$$

The response time of a photodetector is another important characteristic of the device. It is limited by the time it takes for the carriers to cross the depletion region. The response time for silicon detectors is usually 0.5 to 1 nsec, While it is from 1 to 3 nsec for InGaAs detectors. We can reduce the response time by making the intrinsic region as small as possible, but that directly affects the responsivity which is proportional to the size of the intrinsic region, and the thinner the I region is the higher the device capacitance. Capacitance is important for the design of a high speed, low noise detector circuit. It depends on the area of the I region, the thickness of the depletion region and the dielectric constant of the material.

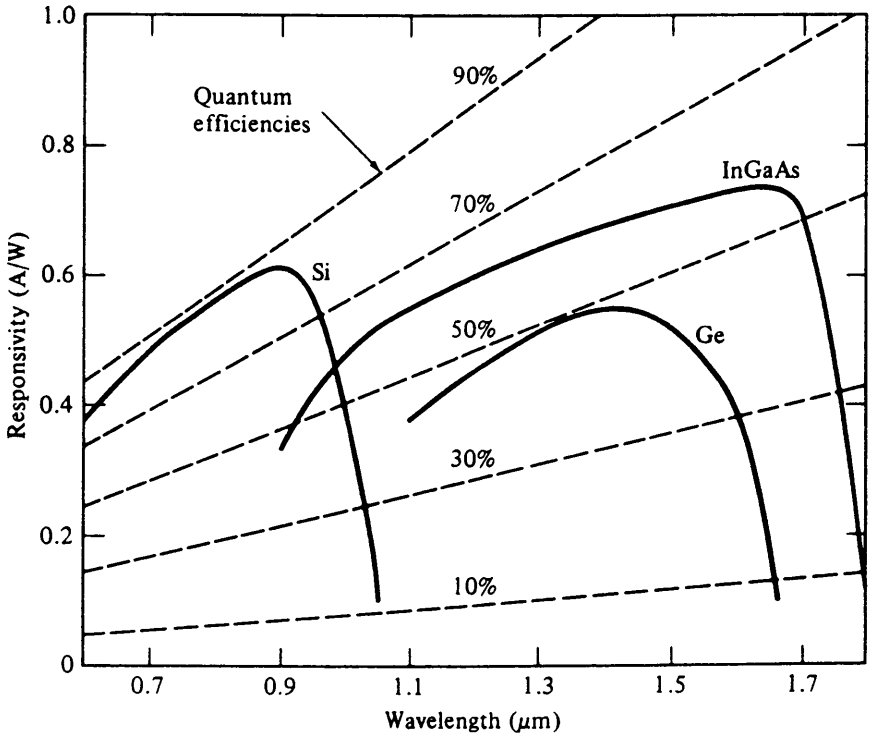

Figure 20

PIN diode responsivity. [12]

5.2 AVALANCHE PHOTODIODES

The second type of photodetectors are the APD's. The doping levels of an APD chip are adjusted to create a region around the junction where the electric field is extremely high under reverse bias conditions. A schematic of a typical APD is shown in Figure 21.

Light is absorbed in the intrinsic type region, and produces electron-hole pairs that find their way into the high field region. In the high electric field region, the electrons are accelerated and impact ionization ogcurs which produces additional electron-hole pairs that contribute to the over all current flowing through the detector. This phenomenon is referred to as the avalanche effect. The ionization collisions created by the avalanche effect translate into a amplification of power.

A major drawback of APD's is the fact that the amplification of power is largely dependent on temperature. High temperature reduces the chance of obtaining ionization collisions and achieving the avalanche effect.

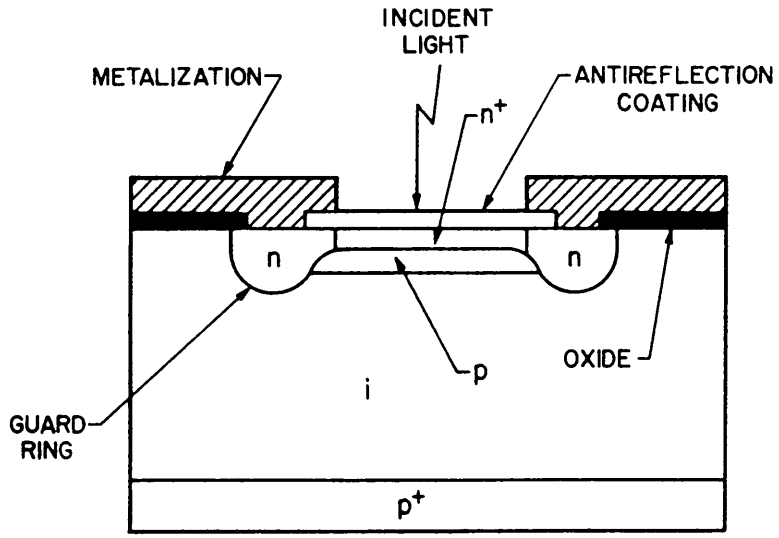

Figure 21

Avalanche photodiode configuration. [27]

6.0 WAVELENGTH SENSITIVE COMPONENTS

6.1 MULTIMODE WAVELENGTH DIVISION MULTIPLEXERS

One of the most popular dual channel wavelength divsion multiplexers in the multimode domain is shown in Figure 22. It is manufactured using two quarter pitch Selfoc lenses and a dichroic filter [10],[15],[19]. The filter is basically a dielectric thin-film stack deposited on a glass substrate. This device contains high and low refractive index dielectric films in alternating layers. Each layer has an optical thickness of approximately one quarter or half wavelength [11].

Light incident on the filter suffers successive refractions off of the different layers. The light is then broken down into a passband and a stopband.

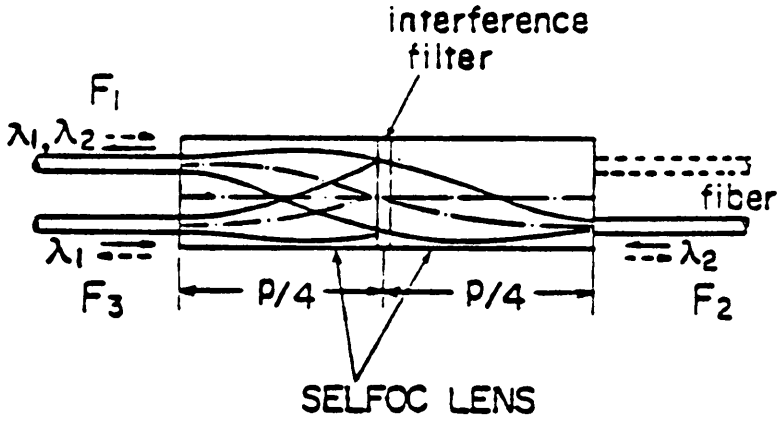

Figure 22

Multimode WDM with Selfoc lens and dichroic filter. [21]

The passband is transmitted through the filter, and is basically the addition of all wavelengths that were transmitted. The stopband is reflected from the filter and is basically the sum of the reflected wavelengths that destructively interfered. There is close to no absorption in the dichroic filter, so the percentage reflected is 100 minus the percentage transmitted. A plot of a typical spectral response of a band-pass filter at normal incidence is shown in figure 23.

Dichroic filters are fabricated using an electron beam that evaporates highly stable materials such as SiO_2 (n= 1.46) and TiO_2 (n=2.3). Long wave pass (LWP) and short wave pass (SWP) filters are also manufactured using the same technique.

The left quarter-pitch Selfoc lens of Figure 22 forms a collimated beam at the filter, and provides normal incidence. The light beam has to be collimated in between the two lenses because a non-collimated beam would suffer excessive divergence, and the WDM becomes too lossy. The right Selfoc lens converges the light onto fiber number 3 and enables us to gather close to 95% of the incident beam after it goes through the filter.

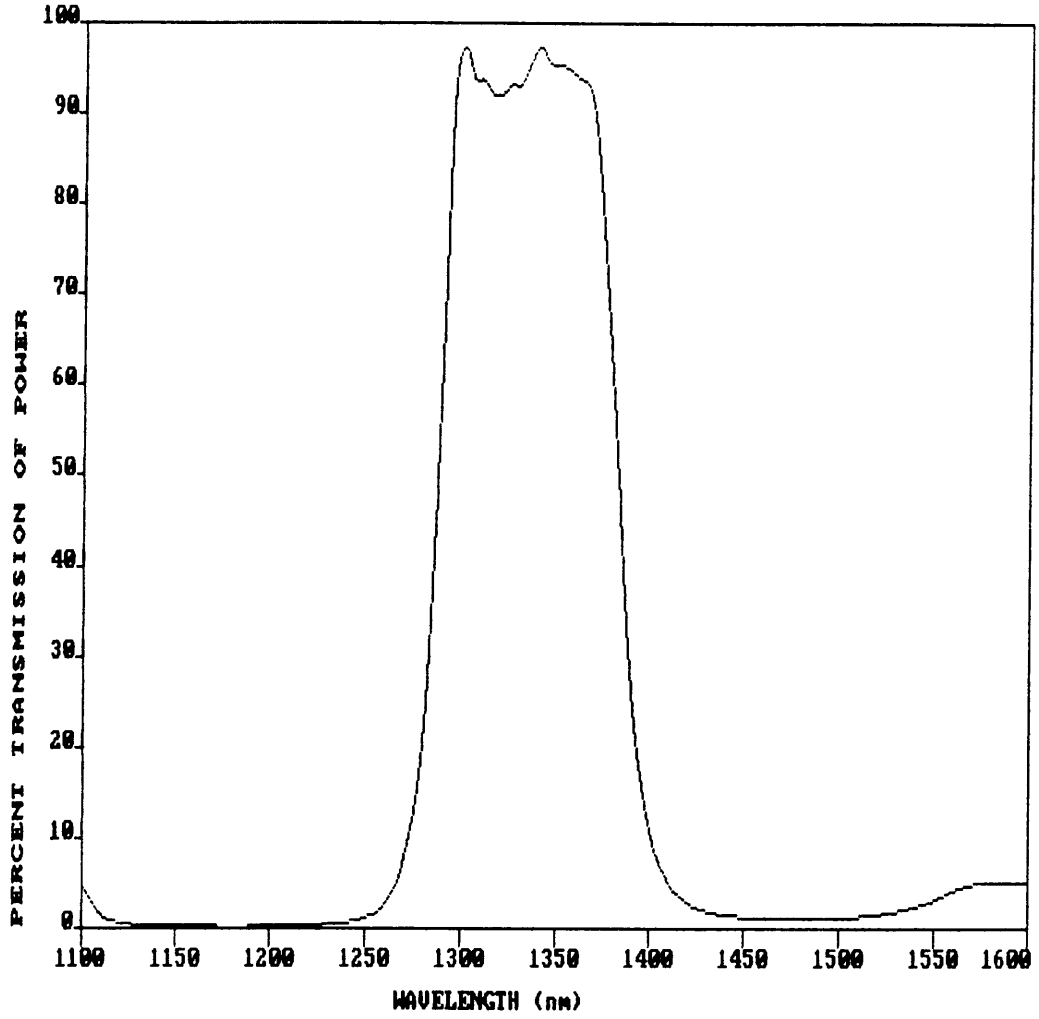

Figure 23

Spectral response of a 1300 nm dichroic band pass filter.

The index of refraction of the Selfoc lens (Figure 24) is given by:

$$N(r) = N_0 \left(1 - \frac{A}{2} r^2 \right) \qquad (6\text{-}1)$$

where N_0 = Refractive index on axis.

A = Refractive index gradient constant.

The transmission of an optical ray with initial slope θ_1 and radial displacement r_1 through a Selfoc lens is given by the following [21]:

$$\begin{bmatrix} \theta_1 \\ r_1 \end{bmatrix} = \begin{bmatrix} \cos(2\pi p) & -N_0\sqrt{A}\,\sin(2\pi p) \\ (N_0\sqrt{A})^{-1}\sin(2\pi p) & \cos(2\pi p) \end{bmatrix} \begin{bmatrix} \theta_2 \\ r_2 \end{bmatrix} \qquad (6\text{-}2)$$

The distance between the focal point and the end surface is:

$$s = \frac{1}{N_0\sqrt{A}\,\tan(2\pi p)} \qquad (6\text{-}3)$$

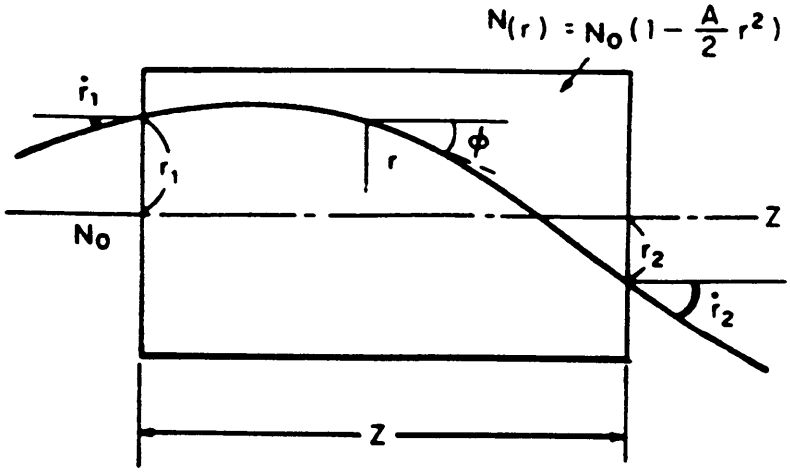

Figure 24

Selfoc lens. [21]

The pitch is related to the length of the lens by the following equation:

$$2\pi p = Z \sqrt{\vec{A}} \qquad (6\text{-}4)$$

6.2 SINGLE MODE WAVELENGTH DIVISION MULTIPLEXERS

Microoptic components such as lenses, gratings and dielectric filters are not very easy to use in single mode fiber optic systems due to:

* chromatic aberrations in lenses and gratings

* difficulty in producing such components with high precision required for single mode use

* extremely hard to align

It is very advantageous if we can perform the wavelength division multiplexing while keeping the light$within the fiber. We know that by placing two fibers close enough to each other, so that they lie in the evanescent field

region, power is coupled from one to the other. Standard single mode splitters are fabricated with this same concept. They are manufactured by etching part of the cladding off, twisting the fibers over each other and fusing while stretching them to make a fused biconic taper coupler [13]. Another method involves etching, polishing part of the cladding off, and fusing the fibers, and thus providing the narrow spacing between the two cores.

A single mode wavelength division multiplexer is manufactured pretty much the same way, but with two slightly different fibers [18],[23],[24]. Figure 25 shows a typical fused all-fiber WDM. Maximum coupling between two forward traveling modes is possible when the propagation constants of the modes β_1 and β_2 are equal. By choosing two fibers that have similar β's only at the wavelength that we would like to achieve power coupling, then we can come up with a coupler that is wavelength dependent.

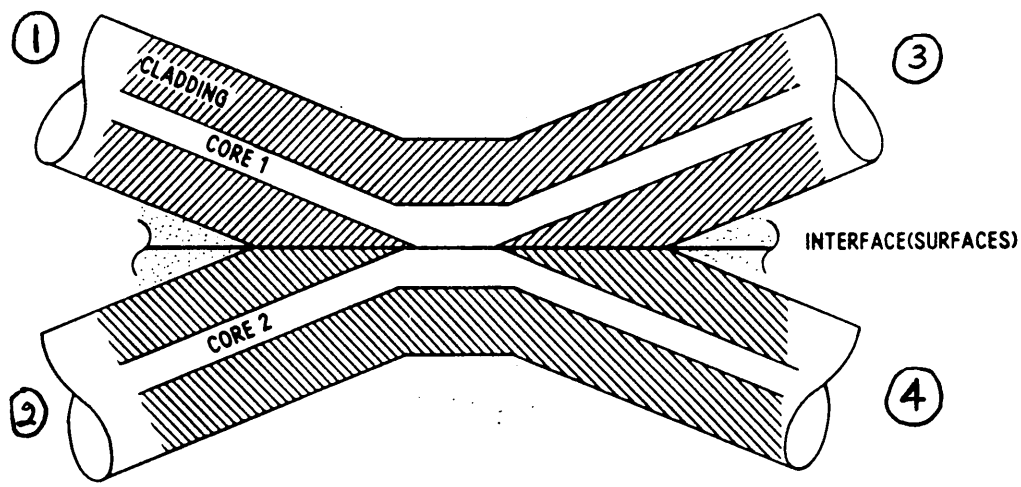

Figure 25

Single mode

wavelength division multiplexer. [27]

The insertion loss of single mode wavelength division multiplexers is usually less than 0.5 dB which makes them very attractive for long distance and high bit rate communication [17]. The wavelength isolation is around 15 to 20 dB which is usually not high enough for high speed communication [25]. The addition of filters is required to achieve low crosstalk. With the all-fiber design, these devices are environmentally very stable, and allow the user to deploy them in harsh environments. Special care has to be exercised when packaging these single mode WDM's because any bending of the coupling region would have dramatic effects on insertion loss and wavelength isolation.

6.2.1 COUPLED MODE THEORY

The coupled mode equations ([1],[2],[20],[22],[26]) in the case of two single mode fibers reduce to the following equations:

$$\frac{dA_1}{dz} + i\,\beta_1 A_1 = i\,C_{12}A_2 \qquad (6\text{-}5)$$

$$\frac{dA_2}{dz} + i\,\beta_2 A_2 = i\,C_{21}A_1 \qquad (6\text{-}6)$$

where A_1 and A_2 are the amplitudes of the modes and β_1 and β_2 are the propagation constants. C_{12} and C_{21} are the coupling coefficients. If mode 1 is normalized to an initial unit power, and mode 2 to zero power. Then the solution to equations (6-5) and (6-6) is:

$$|A_1|^2 = 1 - F_{12} \sin^2\beta_b z \tag{6-7}$$

$$|A_2|^2 = F_{21} \sin^2\beta_b z \tag{6-8}$$

where for forward moving modes:

$$F_{12} = \left[1 + \frac{(\beta_2-\beta_1)^2}{4|C_{12}C_{21}|} \right]^{-1} \tag{6-9}$$

$$F_{21} = \left| \frac{C_{21}}{C_{12}} \right| F_{12} \tag{6-10}$$

$$\beta_b = \left[\frac{|C_{12}C_{21}|}{F_{12}} \right]^{\frac{1}{2}} \tag{6-11}$$

The power transfer takes place over a distance

$$L = \frac{\pi}{2\beta_b} \tag{6-12}$$

When $\beta_1 = \beta_2$, $C_{12} = C_{21}$, $F_{12} = F_{21}$, $\beta_b = |C_{12}|$ and power transfer is maximum. For modes traveling in the opposite direction, the difference in propagation constants is very large and extremely low coupling occurs.

6.2.2 EXPERIMENTAL MEASUREMENTS OF SINGLE MODE WDM'S

The coupling ratio of a 1300/1550nm single mode WDM is shown in Figure 26. The coupling ratio, CR, is defined as:

$$CR = \frac{\text{Output power at port 1}}{\text{Output at port 1 + Output at port 2}} \qquad (6\text{-}13)$$

The loss through the WDM is shown in Figure 27. The loss is defined as:

$$\text{Loss (dB)} = -10\log\left[\frac{\text{Output at 3 + Output at 4}}{\text{Input power at port 1}}\right] \qquad (6\text{-}14)$$

The directivity which is a measure of coupling between oppositely moving modes was measured to be larger than 50 dB when both ports 3 and 4 were index matched.

The directivity is given by:

$$\text{Directivity} = -10\log\left[\frac{\text{Output at port 2}}{\text{Input at port 1}}\right] \qquad (6\text{-}15)$$

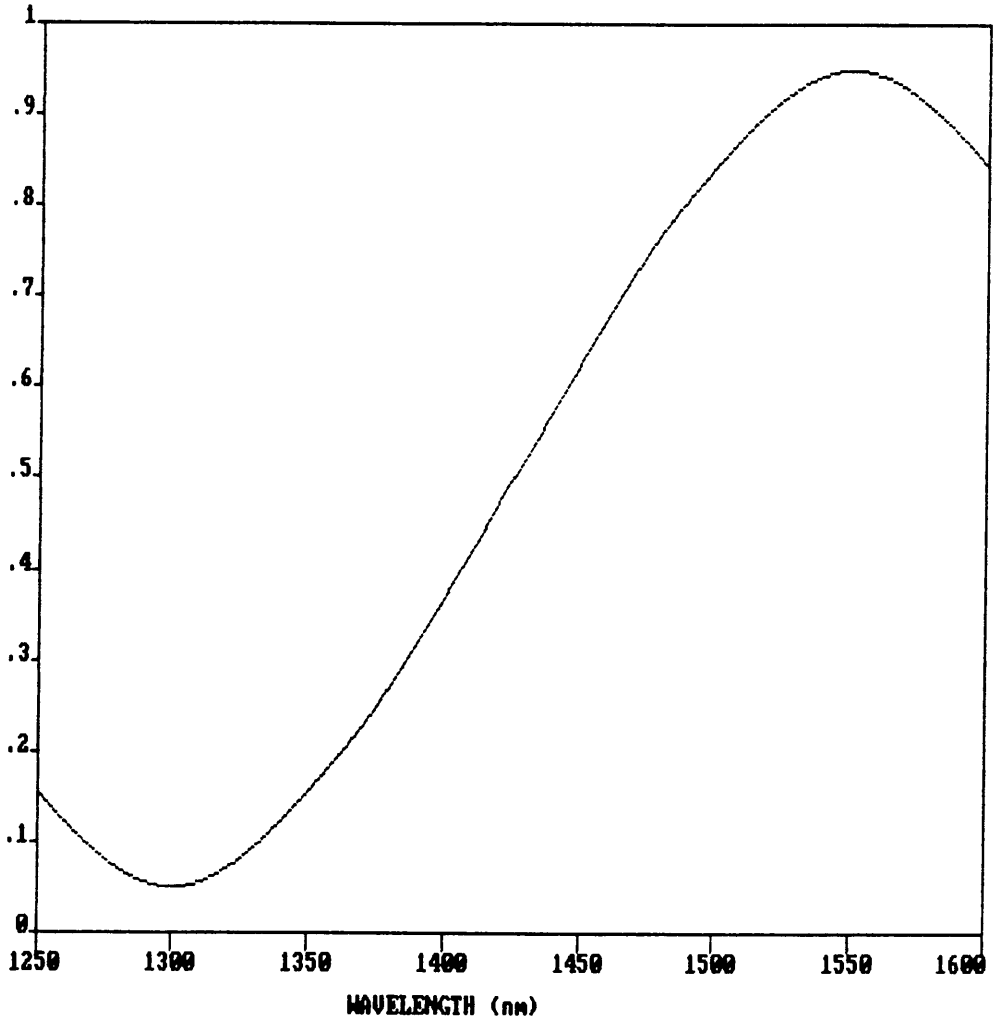

Figure 26

Coupling ratio of a 1300/1550 nm
single mode wavelength division multiplexer.

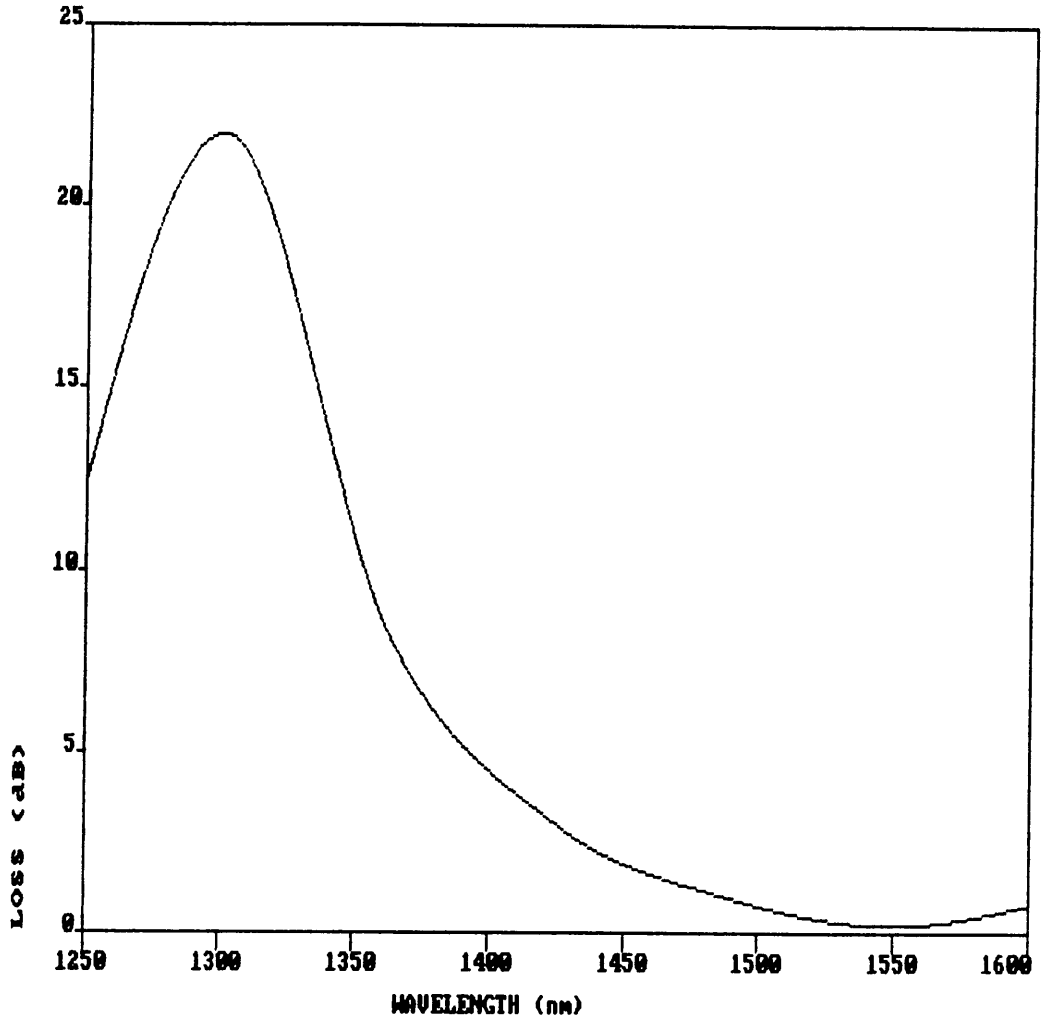

Figure 27

Loss through a

1300/1550 nm single mode WDM

7.0 ATTENUATION

Attenuation in optical fiber is due to power absorption, the presence of OH ions and scattering. Absorption is caused by defects in the fiber, impurities in the glass material and the basic materials of which fibers are made. The Rayleigh scattering loss in optical fibers along with the absorption loss in the ultraviolet region define the optical loss at low wavelength from 700 to 1200 nm. Above 1200 nm, the absorption loss in the infrared region takes over, and in between we find attenuation peaks due to absorption caused by the presence of the OH ion. These peaks occur at 725, 950 and 1400 nm. The largest attenuation is at 1400 nm.

Fiber loss in the 800 nm window ranges from 5 to 2.5 dB/km. The attenuation in the 1300 nm region is usually less than 0.5 dB/km, and the loss in the 1500 nm window is usually less than 0.3 dB/km.

Power is lost in cabling the fiber which introduces bends along the fiber length. Connectors and splices also contribute to the overall attenuation of the optical signal.

A very important feature in optical connectors is the possibility of having a physical contact between the two mating cores. Contact is achieved by polishing the ferrules to a convex surface, and having a spring loaded mechanism to push the fibers together. Single mode connectors with physical contact, like the NTT FC/PC type reduce optical loss to 0.2 dB. Flat ended connectors have an air gap between the cores, and suffer from Fresnel reflections. With physical contact single mode connectors, power reflection is reduced to at least 25 dB below incident power as compared to 14 dB in flat polished connectors. Power reflection from connectors is of great importance when it comes to wavelength division multiplexing because it results in high crosstalk between channels, and reduces the signal to noise ratio.

8.0 BANDWIDTH

As a signal is transmitted along the fiber it suffers from degradation due to chromatic and intermodal dispersion. Chromatic or intramodal dispersion is signal degradation within a single mode. It is divided into two phenomena, the first is material dispersion which is due to the effect that that the index of refraction of the optical fiber is a function of wavelength. The second is waveguide dispersion which is caused by the fact that the propagation constant β is a function of the core size and the wavelength. The rise time due to material dispersion is :

$$t_m \text{ (psec)} = L\sigma D_m \qquad (8\text{-}1)$$

where L = distance in km

σ = spectral width of source in nm

D_m = material dispersion in psec/(nm.km)

The rise time due to waveguide dispersion in step index fibers is given by (Figure 28):

$$t_w = - \frac{n_2 L \Delta \sigma}{c \lambda} V \frac{d^2(Vb)}{dV^2} \qquad (8\text{-}2)$$

Intermodal dispersion is present in multimode fibers, and causes signal distortion because different modes travel with different velocities along the fiber. Graded index fibers suffer much less intermodal dispersion, and their bandwidth distance product is considerablly higher than that of step index fibers.

The rise time due to intermodal dispersion in step index multimode fibers is given by:

$$t_{mod} \text{ (nsec)} = \frac{440\ L^q}{B_0} \qquad (8\text{-}3)$$

where B_0 = bandwidth of a 1 km length of cable in MHz

$0.5 \leq q \leq 1.0$, usually $q = 0.7$

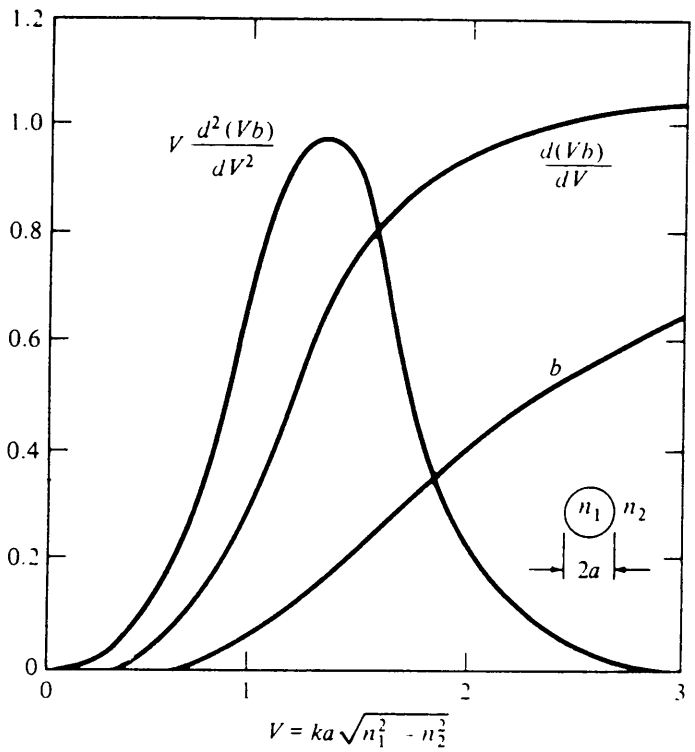

Figure 28

V*d^2(Vb)/dV^2 as a function of V. [12]

The overall system risetime is given by:

$$t_s = \sqrt{t_t^2 + (t_m+t_w)^2 + t_{mod}^2 + t_r^2} \qquad (8\text{-}4)$$

where t_r = rise time of receiver

t_t = rise time of transmitter

Coding schemes play a very important role in determining the bandwidth of the system. Return to zero, RZ, non return to zero, NRZ, and mBnB block codes are common coding schemes in optical fiber communication. By choosing the more complex mBnB block codes or Manchester data coding data, can be transmitted with a reletively low bit error rate at a slightly higher bandwidth requirement.

9.0 SYSTEM DESIGN

In this chapter, we design a 20 km dual channel wavelength division multiplexing datalink.

9.1 SYSTEM SPECIFICATION

The project involves having optical fiber cable reaching the home, with the local telephone company handling telephone lines, computer data transmission and TV channels (Figure 29)[4]. Fiber-to-the home is a fairly efficient way of having both TV and phone signals on one fiber. The consolidation of home communication is thought to become part of our near future. The communication channel from the home to the distribution center ms as follows:

Maximum bit rate : 0.5 Mbit/sec

Description : telephone lines and computer data transmission

The communication channel from the distribution center to the home is as follows:

Maximum bit rate : 150 Mbit/sec

Description : telephone lines, computer data transmission and TV channels

The local phone company would like to lay single mode (9/125 μm fiber) cable in the ground because of possible upgrades in the near future, one being high definition TV (HDTV) with data rates reaching 1 Gb/sec. The link is required to have 7 splices and 7 connectors.

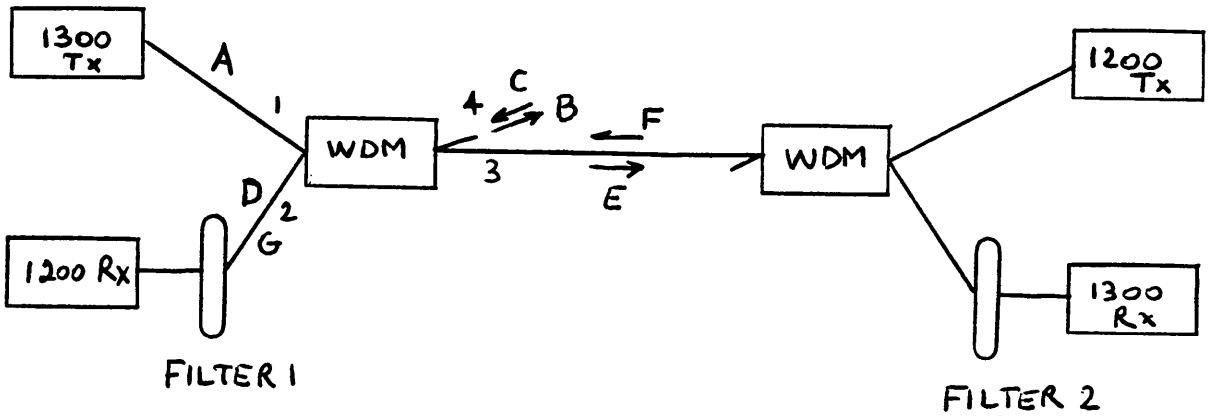

Figure 29

Proposed datalink

9.2 HIGH SPEED CHANNEL POWER AND BANDWIDTH BUDGETS

With the 150 Mbit/sec data rate, we immediately think of having a laser in the 1300 nm window to serve the channel from the distribution center to the home. The available receiver sensitivity at 150 Mbit/sec and a BER of 10^{-9} is -32.0 dBm if we use an InGaAs PIN photodiode.

The power budget at 1300 nm is :

Component	Power / Loss dB
Laser	0 dBm
50% Duty Cycle	-3.0
WDM	-0.5
Cable (0.6 dB/km)	-12.0
Splicew (0.3 dB each)	-2.1
Connectors (0.5 dB each)	-3.5
WDM	-0.5
Filter	-1.5
Minimum received power :	-23.1
Margin :	-6.0
Required sensitivity :	-29.1 dBm
Available sensitivity :	-32.0 dBm

The rise time of the fiber is due to both material and waveguide dispersion. The material dispersion at 1300 nm is 5 ps/(nm.km). It causes a rise time t_m = 0.4 nsec for a 1300 nm laser with 4.0 nm spectral width. The waveguide dispersion rise time t_w = 0.3 nsec if we consider n_2 = 1.5, the index difference = 0.01 and $V*d^2(Vb)/dV^2$ = 0.1.

The rise time budget is:

Component	Rise time (nsec)
Transmitter	3.0
Fiber ($t_m + t_w$)	0.7
Receiver	3.3
System Rise Time :	4.5 nsec
Available Rise Time (NRZ) :	4.67 nsec

9.3 LOW SPEED CHANNEL POWER AND BANDWIDTH BUDGETS

The choice of the second wavelength for the low data rate channel is somehow undefined. The loss of the single mode fiber cable at 800 nm is around 3.5 dB/km. With such a loss we can definitely not work with an 850 nm source because it

would require a link budget greater than 70 dB. At 1200 nm the loss of the fiber cable is approximately 0.65 dB/km. With such a low loss, we can use an LED coupled to a single mode fiber (9/125 μm). It is preferable to stay away from the 1500 nm window even though the attenuation is very low. 1500 nm sources are extremely expensive, but it would be feasable to use them if all other less expensive options fail. The available receiver sensitivity at 0.5 Mbit/sec and a BER of 10^{-9} is -56.0 dBm for an InGaAs PIN.

The power budget at 1200 nm is as follows :

Component	Power / Loss dB
LED	-23.0 dBm
50% Duty Cycle	-3.0
WDM	-1.5
Cable (0.65 dB/km)	-13.0
Splices (0.3 dB each)	-2.1
Connectors (0.5 dB each)	-3.5
WDM	-1.5
Filter	-1.5

Minimum received power :	-49.1 dBm
Margin :	-6.0
Required sensitivity :	-55.1 dBm
Available sensitivity :	-56.0 dBm

The rise time of the fiber is due to both material and waveguide dispersion. The material dispersion at 1200 nm is 10 ps/(nm.km). It causes a rise time t_m = 10.0 nsec for a 1200 nm LED with 50 nm spectral width. The waveguide dispersion rise time t_w = 3.3 nsec if we consider n_2 = 1.5, the index difference = 0.01 and $V*d^2(Vb)/dV^2$ = 0.08.

The rise time budget is:

Component	Rise time (nsec)
Transmitter (max)	400
Fiber (t_m + t_w)	13.3
Receiver (max)	500
System Rise Time :	640 nsec
Available Rise Time (RZ) :	700 nsec

9.4 CROSSTALK ANALYSIS

The mechanism of crosstalk in a single mode wavelength division multiplexer is dependent on the reflection from the 4th unused port, reflection from connectors and splices and the out of band emmission of the sources. Figure 29 shows the system to be implemented. Because of the close

spacing of the wavelength we would require the use of thermoelectric coolers to maintain the wavelength to within ± 5 nm.

9.4.1 CROSSTALK AT THE DISTRIBUTION CENTER

The signals are expressed in dB, and they are indicated by capital letters. A is the output power spectrum from the 1300 nm laser (Figure 17 for example). B is the signal at port 4 of the WDM.

$$B = A - WDM_{14} \qquad (9\text{-}1)$$

where: WDM_{14} is the response of the WDM with input at port 1 and output at port 4 (Figure 30).

Port 4 of the WDM is not connected to anything, so according to Fresnel reflection, power is reflected back at the glass air interface. In order to reduce the reflected power, port 4 is usually terminated with index matching epoxy that provides reflection losses of 25 dB or more. The reflected power C is then:

$$C = B - 25\ dB \qquad (9\text{-}2)$$

$$D = C - WDM_{42} \quad (9\text{-}3)$$

D is the crosstalk caused by the presence of the 1300 nm laser and the WDM. Let us define the near end crosstalk system response, XNE to be:

$$D = A - XNE \quad (9\text{-}4)$$

This implies that:

$$XNE = WDM_{14} + WDM_{42} + 25\ dB \quad (9\text{-}5)$$

Let E be the signal at port 3 of the WDM.

$$E = A - WDM_{13} \quad (9\text{-}6)$$

$$F = E - \Sigma \text{ connector, splice and cable reflections} \quad (9\text{-}7)$$

The power reflection from physical contact connectors is 25 dB below incident power. Note that the contribution of any connector or splice 20 km away in our system is negligible. Let G be the crosstalk signal caused by the presence of connectors, splices and cable.

$$G = F - WDM_{32} \quad (9\text{-}8)$$

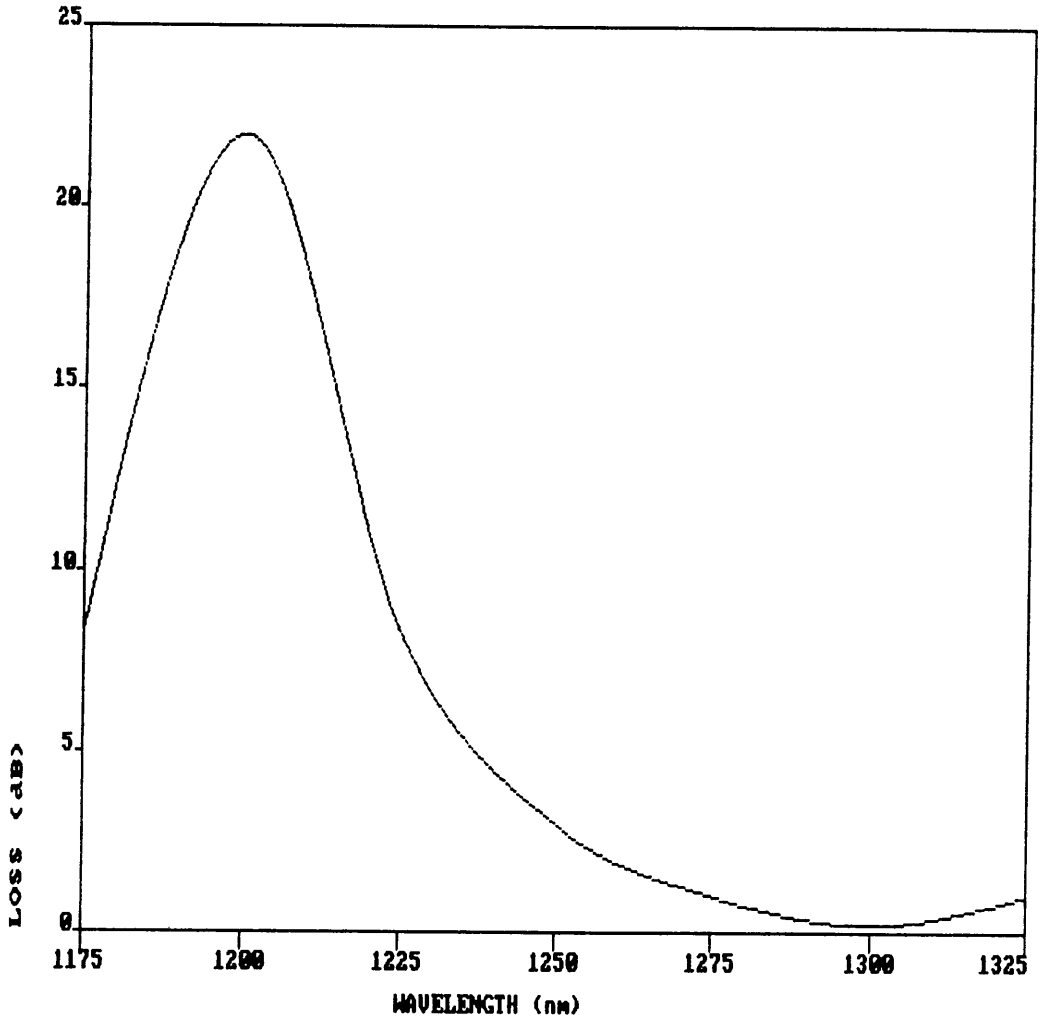

Figure 30

Loss through a

1200/1300 nm single mode WDM.

Let us now define the far end crosstalk system response, XFE to be:

$$G = A - XFE \tag{9-9}$$

$$XFE = WDM_{13} + WDM_{32} + \hat{E}\ \text{Reflections} \tag{9-10}$$

Since the single mode wavelength division multiplexer is bidirectional then

$$W = (WDM_{13} + WDM_{32}) = (WDM_{14} + WDM_{42}) \tag{9-11}$$

The total crosstalk at the distribution center is the sum of both the near end and far end crosstalks. Either the far end or the near end can be the dominant crosstalk channel depending on the reflection from port 4 of the WDM, and the connectors. In our case, the sum of the reflections from the connectors is estimated to be 18 dB. Then the total crosstalk, XTALK with A from Figure 17 is: (Figure 31)

$$XTALK = A - W - 17.2\ dB \tag{9-12}$$

The integration of the crosstalk over the wavelength from 1300 to 1330 nm yields -33 dBm of total unwanted signal. Since the signal into the 1200 nm detector is as low as

-56 dBm, then we would require the use of a filter. The filter should be 95% transmissive from 1150 to 1250 nm, and it should have an isolation equal to 43 dB from 1280 to 1350 nm. A filter like that would maintain a signal to noise ratio equal to 20 dB.

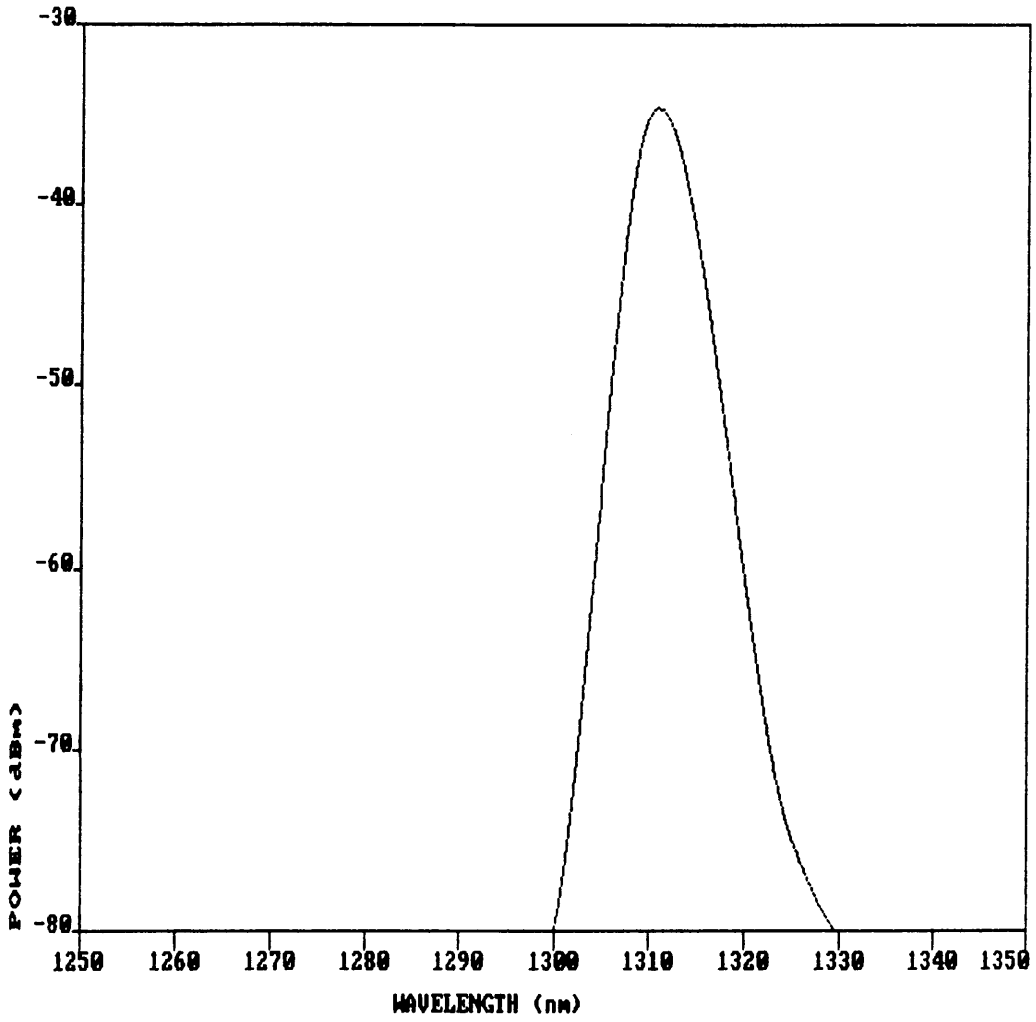

Figure 31

Total crosstalk at the

distribution center.

9.4.2 CROSSTALK AT THE RESIDENCE

The analysis is exactly the same as above, and the total crosstalk is given by equation (9-12) except that now A is the spectral output of a 1200 nm LED (Figure 32). Figure 31 shows the total crosstalk at the residence relative to the output power of the 1200 nm LED. The total unwanted signal integrated over the wavelengths from 1100 to 1300 nm turns out to be 17 dB below a output power of 5 W. This implies that the crosstalk power level is -40 dBm as compared to a signal power of -29 dBm.

The filter should be 95% transmissive from 1290 to 1320 nm, and it should have an isolation equal to 10 dB from 1100 to 1270 nm. The signal to noise ratio with the filter would be in excess of 20 dB. We notice that the crosstalk power at a wavelength of 1270 nm or more would not be filtered. It is not a problem in this case, but it could be if the spectral width of the LED was much larger.

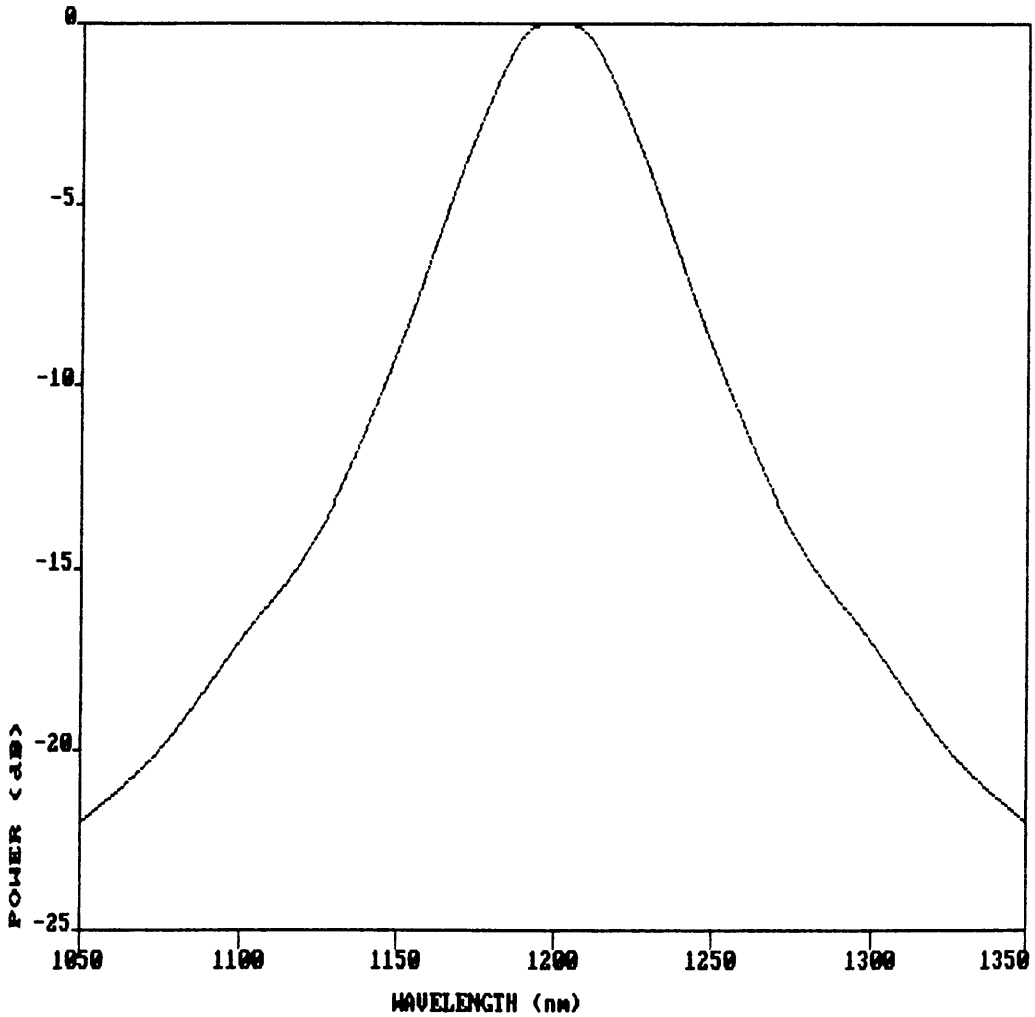

Figure 32

Spectral output of a 1200 nm LED coupled to a 9/125 µm fiber.

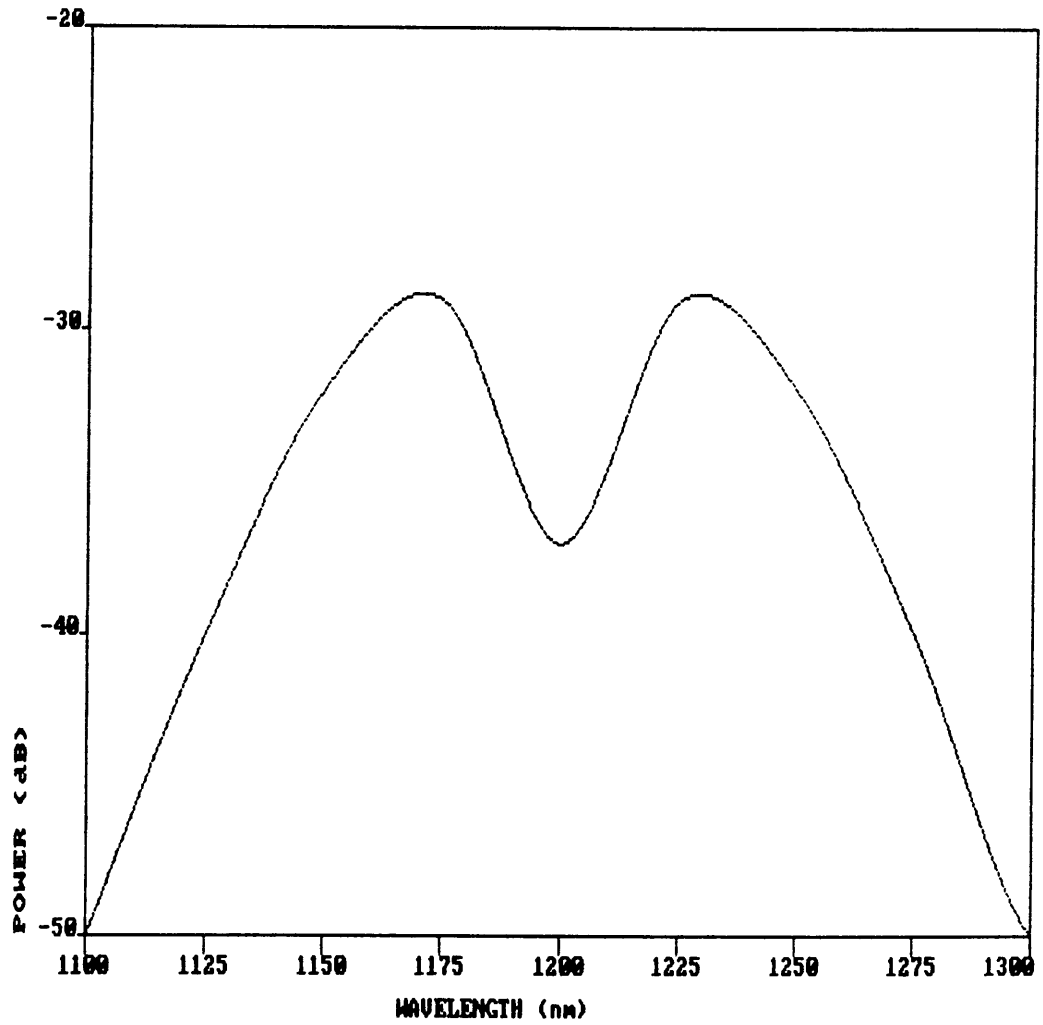

Figure 33

Total crosstalk at the residence.

10.0 CONCLUSIONS

In the thesis we covered the important elements for designing a bidirectional wavelength division multiplexing datalink which are:

* lasers and LED's and their output spectrum
* detectors
* dual channel WDM's both single mode and multimode
* fiber and cable

A 20 km, single mode, fiber-to-the home link was designed by first selecting a 1300 nm laser diode to serve the high data rate channel (150 Mb/sec). We chose a 1200 nm LED for the low data rate channel (0.5 Mb/sec). We performed both the power and bandwidth budgets, and then analyzed the crosstalk in order to specify the filters that would provide an optical signal-to-noise ratio of 20 dB.

If we define the total reflections, REF to be:

$$REF = -10 \log (\text{Reflections from connectors and splices} + \text{Reflection at port 4 of WDM}) \quad (10\text{-}1)$$

and ignore the effect of the directivity of the single mode WDM because it was measured to be 50 dB. The total crosstalk for our proposed datalink configuration (Figure 29) is given by:

$$XTALK = A - W - REF \quad (dB) \quad (10\text{-}2)$$

where A is the source output spectrum of the opposite channel, and W is given by equation (9-11).

We concluded that a filter with minimum isolation of 43 dB is required at the distribution center while a filter with minimum isolation of 10 dB is required at the residence. There was no need in our design to consider the changes of the detector responsivity with respect to wavelength because the center wavelengths of both channels were close to each other. In the case of interwindow wavelength division multiplexing, the total crosstalk equation becomes:

$$XTALK = A - W - REF + 10 \log (R_1 - R_2) \quad (dB) \qquad (10\text{-}3)$$

where R_1 is the responsivity at the wavelength of the signal and R_2 is the responsivity at the wavelength of the noise source.

Our analysis and design may be extended to multichannel and unidirectional WDM datalinks.

REFERENCES

[1] SNYDER, A W., Coupled-Mode Theory for Optical Fibers. Journal Of The Optical Society Of America, Vol 62 No.11, 1267-1277, November 1972.

[2] MCINTYRE, P D. and A W SNYDER., Power Transfer Betweem Optical Fibers. Journal Of The Optical Society Of America, Vol 63 No.12, 1518-1527, December, 1973.

[3] NOSU, K and H ISHIO, A Design Of Multiplexers For Optical Wavelength-Division Multiplexing Transmission Via A Single Fiber. Proceedings of 1979 ISCAS, 735-738, 1979.

[4] HARA, E.H., K.O. Hill, B.S. KAWASAKI and D.C. JOHNSON, The Use Of An Optical Power Combiner For Multiplexing Multiple Television Sources In Single-Fiber Optical Systems. IEEE Transactions on Cable Television, Vol.CATV-4 No.2, 49-55, April 1979.

[5] BLISS, J., Basic Concepts Of Fiber Optics And Fiber Optic Communications. Application Note AN-846, Motorola Semiconductor Products Inc..

[6] ADAMS, M.J., An Introduction To Optical Waveguides. John Wiley & Sons, 1981.

[7] SZE, S.M., Physics of Semiconductor Devices. John Wiley & Sons, 1981.

[8] WILLIAMS, J C. and S E. GOODMAN, Fiber Optics Wavelength Division Multiplexing For Aircraft Applications. Proceedings Of The IEEE 1982 National Aerospace and Electronics Conference (NAECON), 833-840, 1982.

[9] MARCUSE, D., Light Transmission Optics, Second Edition. Van Nostrand Reinhold, 1982.

[10] LIPSON, J. and G. T. HARVEY, Low-Loss Wavelength Division Multiplexing (WDM) Devices for Single-Mode Systems. Journal of Lightwave Technology, Vol. LT-1 No. 2, 387-390, June 1983.

[11] BANDETTINI, S. P., Optical Filters for Wavelength Division Multiplexing. Optical Coating Laboratory, Inc., April 7, 1983.

[12] KEISER G., Optical Fiber Communications. McGraw-Hill Book Company, 1983.

[13] WINZER, G., Wavelength Multiplexing Components- A Review of Single-Mode Devices and Their Applications. Journal of Lightwave Technology, Vol. LT-2 No. 4, 369-378, August 1984.

[14] KAPRON, F. P., Critical Reviews of Fiber-Optic Communication Technology: Optical Fibers. SPIE Vol. 512, Fiber Optic Communication Technology, 2-16, 1984.

[15] AGARWAL, A. K., Review of Optical Fiber Couplers. Fiber and Integrated Optics, Vol.6 No.1, 27-53, March 7, 1985.

[16] Application Notes For Thermoelectrics Devices. MELCOR Materials Electronic Products Corporation, Trenton, New Jersey.

[17] CORKE, M., K. SWEENEY, R. PRATER, J. MUHS and K. SCHMIDT, Fiber Optic Components for Communication Applications. Amphenol Fiber Optic Products, Lisle, Illinois, 1-11, 1987.

[18] TEKIPPE, V.J., C.M. LAWSON, P.M. KOPERA and T.Y. HSU, Monomode Wavelength Division Multiplexer/Demultiplexer. Gould Research Center, Rolling Meadows, Illinois.

[19] ISHIO, H., J. MINOWA and K. NOSHU, Review and Status of Wavelength-Division-Multiplexing Technology and Its Application. Journal of Lightwave Technology, Vol. LT-2 No.4, 448-463, August 1984.

[20] HARDY, A. and W. STREIFER, Coupled Mode Theory of Parallel Waveguides. Journal of Lightwave Technology, Vol. LT-3 No.5, 1135-1146, October 1985.

[21] The Theory and Design of the SELFOC Lens. NSG America, Inc.

[22] ZENGERLE, R. and O. G. LEMINGER, Wavelength-Selective Directional Coupler Made of Nonidentical Single-Mode Fibers. Journal of Lightwave Technology, Vol. LT-4 No.7, 823-827, July 1986.

[23] CORKE, M., K. L. SWEENEY and K. M. SCHMIDT, Recent Advances in Fiber Optic Coupler Technology. SPIE Vol. 722, Components for Fiber Optic Applications, 2-10, 1986.

[24] SWEENEY, K. L., M. CORKE, B. M. KALE and P. M. KOPERA, Wavelength Dependence of Devices Fabricated in Single Mode Fiber. Amphenol Fiber Optic Products, Lisle, Illinois, 1986.

[25] TEKIPPE, V.J., Fused Wavelength Division Multiplexers/Demultiplexers. Proceedings of OPTO '87, Paris, 192-195, 1987.

[26] SNYDER, A. W. and A. ANKIEWICZ, Optical Fiber Couplers-Optimum Solution for Unequal Cores. Journal of Lightwave Technology, Vol.6 No.3, 463-474, March 1988.

[27] PERSONICK, S. D., Fiber Optics Technology and Applications, Plenum Press, New York, 1985.

The vita has been removed from the scanned document